STATISTICAL ANALYSIS OF AIREP IN SPANISH AIRSPACE (2014-2024)

Technical note 47 of AEMET

Javier MARTÍN MARTÍN

Benito José FUENTES LÓPEZ

Enrique PORTILLA LÓPEZ

Javier DE LUIS CUARTERO

Ignasi MARTÍ MARTÍ

GOBIERNO DE ESPAÑA

VICEPRESIDENCIA TERCERA DEL GOBIERNO

MINISTERIO PARA LA TRANSICIÓN ECOLÓGICA Y EL RETO DEMOGRÁFICO

aemet Agencia Estatal de Meteorología

Published by:

© Ministerio para la Transición Ecológica y el Reto Demográfico
Spanish State Meteorological Agency (AEMET)
Madrid, 2026

Catalogue of Publications of the Central State Administration of Spain:
https://cpage.mpr.gob.es

NIPO: 666-26-012-8
https://doi.org/10.31978/666-26-012-8

Agencia Estatal de Meteorología (AEMET)
C/ Leonardo Prieto Castro, 8
28040 Madrid
http://www.aemet.es/

@Aemet_Esp

https://www.facebook.com/AgenciaEstataldeMeteorologia

STATISTICAL ANALYSIS OF AIREP IN SPANISH AIRSPACE (2014 - 2024)

Technical note 47 of AEMET

Javier MARTÍN MARTÍN[1], Benito José FUENTES LÓPEZ[1], Enrique PORTILLA LÓPEZ[1], Javier DE LUIS CUARTERO [1], Ignasi MARTÍ MARTÍ[2]

[1] *State Meteorological Agency (AEMET)*

[2]*University of Valencia*

jmartinm@aemet.es, bfuentesl@aemet.es, eportillal@aemet.es, jluisc@aemet.es, marmarig@alumni.uv.es

ABSTRACT

A statistical analysis is presented of AIREP reports on turbulence, icing, and mountain waves issued in Spanish airspace between 2014 and 2024. The study includes their temporal distribution (annual and monthly), spatial distribution (by FIR and main mountain systems), as well as the most affected altitudes.

Keywords: AIREP, turbulence, icing, mountain waves, FIR Spain, aeronautical meteorology.

TABLE OF CONTENTS

1. INTRODUCTION

Reports of significant meteorological conditions observed by aircraft in flight, known as Aircraft Reports (AIREP or ARS), are based on meteorological phenomena that compromise flight safety, as reflected in accident statistics associated with icing and turbulence (Eick, 2015a and 2015b). As such, they constitute a valuable source of information for the surveillance and improvement of operational safety. These reports, generated in real time by flight crews, complement other sources of meteorological observation, especially at flight levels where remote sensor coverage is limited.

It is important to note that these reports include a subjective component, as they are based on the perception and assessment of the pilot on board, in addition to the aircraft's own geometry. This qualitative nature can influence the consistency of the reported data, particularly with regard to the intensity and exact location of the meteorological phenomena under analysis.

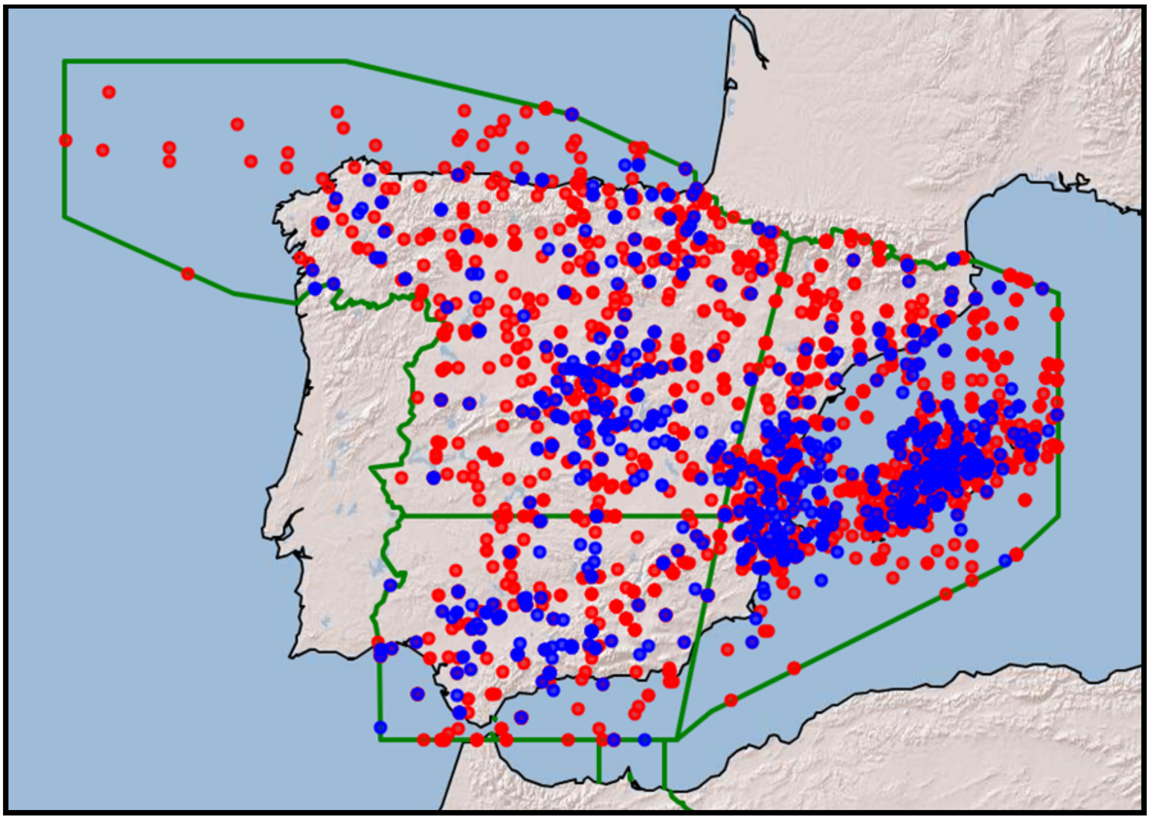

Figure 1. Spatial distribution of the positions of AIREP reports for turbulence (in red) and icing (in blue), period 2014-2024.

This document presents an analysis of AIREP reports related to turbulence and icing phenomena, at moderate (MOD) and severe (SEV) levels, received by the Meteorological Watch Offices (MWO) of AEMET. It includes annual, monthly, and FIR region-segmented (Madrid, Barcelona, and Canary Islands) and mountain system statistics, compiled between 2014 and 2024. Following a rigorous data quality control process, a total of 492 reports were discarded due to typographical errors or incomplete fields, as they prevented automated computation of statistics. Reports whose coordinates fell outside the FIR regions under study were also discarded. As a result, 5 285 AIREP reports associated with icing and turbulence phenomena were compiled, whose spatial distribution is shown in Figure 1 and annual distribution is described in Table 1. Breaking down the reports by intensity, 3200 cases of moderate turbulence (MOD), 1156 of severe turbulence (SEV), 766 of moderate icing (MOD), and 163 of severe icing (SEV) were identified. Additionally, 112 AIREP reports related to mountain waves were identified, of which 99 are recorded within Spanish airspace. Of these, 60 are concentrated within polygons representing the main orographic systems of the Iberian Peninsula.

YEAR	AIREPs	ICE SEV/MOD (%)	TURB SEV/MOD (%)
2014	12	17	83
2015	247	21	79
2016	240	15	85
2017	366	11	89
2018	676	17	83
2019	693	16	84
2020	357	15	85
2021	435	18	82
2022	594	19	81
2023	747	19	81
2024	918	20	80

Table 1. Annual record of AIREPs for Spanish airspace, period 2014-2024.

The positions of the aircraft reports correspond to discrete points defined by codes assigned by ENAIRE, published in its Aeronautical Information Service (AIP) (https://aip.enaire.es/AIP/). Each identifier is associated with a specific geographic location, determined by its latitude and longitude coordinates. For this reason, each point represented in Figure 1 contains a variable number of reports, with a higher concentration near major airports, where air traffic is most intense, primarily during the summer months.

From this it can be observed that there is a stronger correlation between observations and air traffic density than with the actual spatial distribution of the meteorological phenomena causing turbulence and icing. In other words, the spatial distribution of AIREP is conditioned by the concentration of aircraft in certain areas.

Currently, turbulence detection and forecasting rely on more advanced indices, such as the Ellrod1 and Ellrod2 indices (TI1 and TI2), vertical wind shear (VWS), the Richardson number, and the Eddy Dissipation Rate (EDR), which has become the reference standard recommended by the International Civil Aviation Organization (ICAO). At the national level, the MWO in Valencia has developed a specific adaptation for Spanish airspace of a combined and normalized turbulence index described by (Belo-Pereira, 2022). This approach combines various diagnostic indices, including the Ellrod2 index, vertical shear, horizontal deformation, and other predictors derived from the ECMWF's Integrated Forecast System (IFS) numerical model, with the aim of improving the detection of significant turbulence zones.

Recent studies such as (Wen *et al*., 2025) support the idea that icing occurs in the temperature range between –20 °C and 0 °C, with a higher frequency of occurrence in the range between – 10 °C and –2 °C, with severe icing being even more likely in the range between –8 °C and – 2 °C when relative humidity exceeds 65 %. Therefore, the MWO forecasts icing based on the cloud liquid water content between the 0 °C and –15 °C isotherms. In addition, an adaptation of the SFIPO index obtained by (Belo-Pereira, 2015) has been carried out for the IFS numerical model, based on supercooled liquid water content, vertical velocity, relative humidity, and temperature.

For this reason, AIREPs received in real time are of vital importance, as they constitute practically the only direct source for verifying forecasts. Surveillance is also complemented by satellite imagery and derived products obtained through post-processing provided by EUMETSAT's NWC SAF (https://www.nwcsaf.org/).

2. ANNUAL ANALYSIS OF AIREP IN SPANISH AIRSPACE

The combined analysis of AIREP received across the three FIR regions during the period 2014-2024 reveals an evolution marked by sustained growth interrupted only by the impact of the pandemic in 2020 (see Figure 2 and Table A-1). Overall, a significant increase is observed in both moderate and severe phenomena, both reaching their peaks in 2024 with 727 and 191 records respectively.

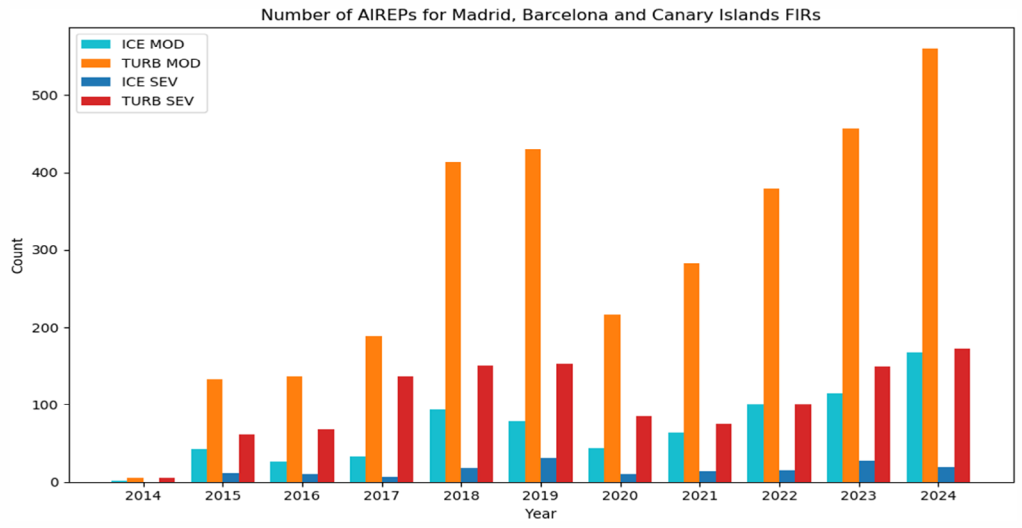

Figure 2. AIREP records for FIR Madrid, Barcelona and Canary Islands, period 2014-2024.

Regarding moderate phenomena, the overall trend is clearly upward. Moderate turbulence accounts for the majority of records, with particularly pronounced growth between 2016 and 2019, and a solid post-pandemic recovery culminating in 2024 with 559 reports. Moderate icing, although in lower volumes, also shows a positive trend, rising from just 2 records in 2014 to 168 in 2024.

Severe phenomena, although less frequent, follow a similar trend. Severe turbulence is the dominant phenomenon in this category, with a peak in 2019 of 153 records and a subsequent steady increase from 2021 to reach 172 records in 2024. Severe icing shows a more irregular evolution, with peaks in 2019 of 31 records and in 2023 of 28, followed by a slight decrease to 19 records in 2024. With regard to icing, the years 2016 and 2019 are particularly noteworthy, as severe reports accounted for approximately 40 % of the number of moderate reports. In the case of severe turbulence, 2017 stands out as especially significant, with severe reports representing 72 % of the moderate reports. Although in 2014 a similar number of severe and moderate turbulence reports were recorded, this result is not considered statistically significant due to the low volume of reports collected that year.

The observed increase in events is strongly related to the recovery of air traffic volumes after the pandemic, as well as the structural limitations of the current AIREP transmission system, which involves flight crews, ENAIRE staff at Area Control Centers (ACC), and AEMET MWO personnel. This procedure, dependent on multiple intermediaries, may introduce variability in the reception and recording of reports. For this reason, it is not possible to establish a direct relationship between the evolution of observations and a real intensification of meteorological phenomena.

2.1 Annual analysis by Flight Information Region (FIR/UIR)

The Flight Information Region (FIR) is an airspace of defined dimensions established by ICAO, from which flight information and alerting services are provided. Spanish airspace, managed by the air navigation service provider (ANSP) ENAIRE, is divided into three FIRs: Madrid, Barcelona, and Canary Islands, whose horizontal boundaries are shown in Figure 1. The Madrid FIR is further subdivided into a northern sub-region managed by the Area Control Center (ACC) of Torrejón de Ardoz (Madrid) and a southern sub-region, whose responsibility falls on the ACC of Seville. The latter also integrates the Melilla Corridor, whose airspace up to flight level FL060 is operationally managed by the Seville ACC. Regarding vertical extent, both the northern and southern sub-regions extend from the surface (SFC) to flight level FL245, and above this limit lie their respective Upper Information Regions (UIR), which cover the upper airspace to unlimited altitude.

During the 2014-2024 period, the majority of the AIREPs analysed were concentrated within the Madrid and Barcelona FIRs, while the Canary Islands FIR made a clearly smaller contribution. Overall, the Madrid and Barcelona FIRs accounted for 94.8 % of the total number of reports, whereas the Canary Islands FIR represented only 5.2 %.

The Madrid FIR, although only slightly exceeding the Barcelona FIR, recorded the highest number of AIREPs during the 2014-2024 period, with a total of 2527 reports, representing 47.8 % of the dataset analysed. As shown in Figure 3 and Table A-2, following the sharp decline recorded in 2020 as a consequence of the COVID-19 pandemic, a sustained recovery was observed, culminating in an annual maximum of 454 reports in 2024.

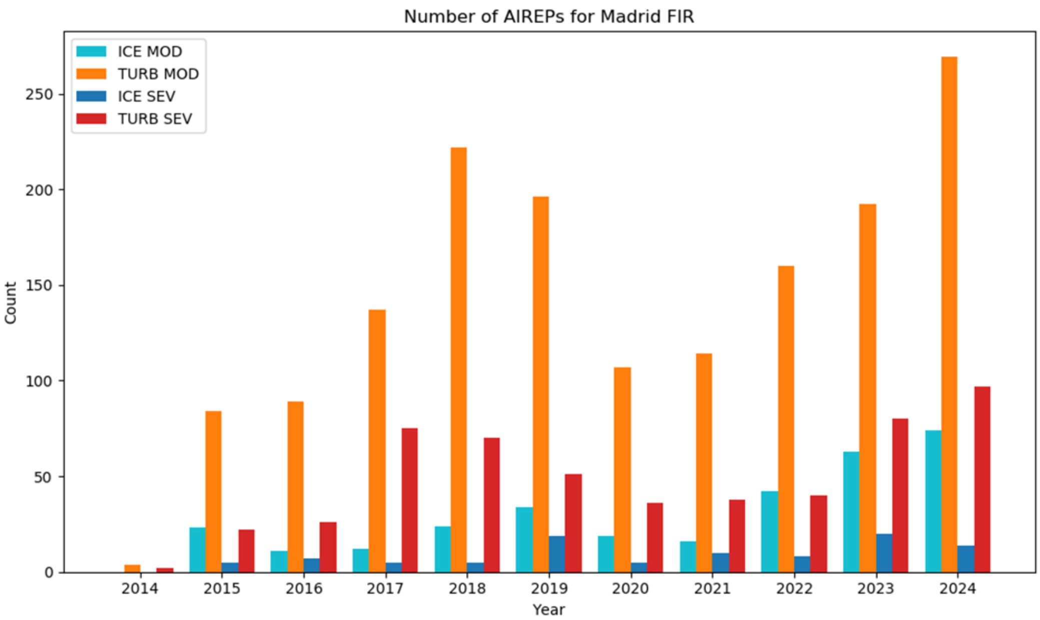

Figure 3. Annual number of AIREPs recorded within the Madrid FIR during the 2014-2024 period.

With regard to moderate turbulence, an absolute maximum was reached in 2024 with 269 reports, exceeding the previous peak recorded in 2018 (222 reports). The evolution of severe turbulence followed a similar trend, with a relative maximum in 2017 (75 reports) and a subsequent increase culminating in 2024 with 97 reports, the highest value of the study period.

Regarding moderate icing, progressive growth was observed from 2019 (34 records) to 74 in 2024. In the case of severe icing, the relative maximum of 2019 stands out (19 records), followed by a post-pandemic rebound leading to the absolute maximum in 2023, with 20 records.

The Barcelona FIR recorded a total of 2 485 AIREPs during the 2014-2024 period, representing 47.0 % of the total dataset analysed. Its interannual evolution was very similar to that observed in the Madrid FIR (see Figure 4 and Table A-3). A peak was recorded in 2019, with 389 reports, followed by a marked decline in 2020 as a consequence of the COVID-19 pandemic. This was followed by a gradual recovery, culminating in 349 reports in 2024.

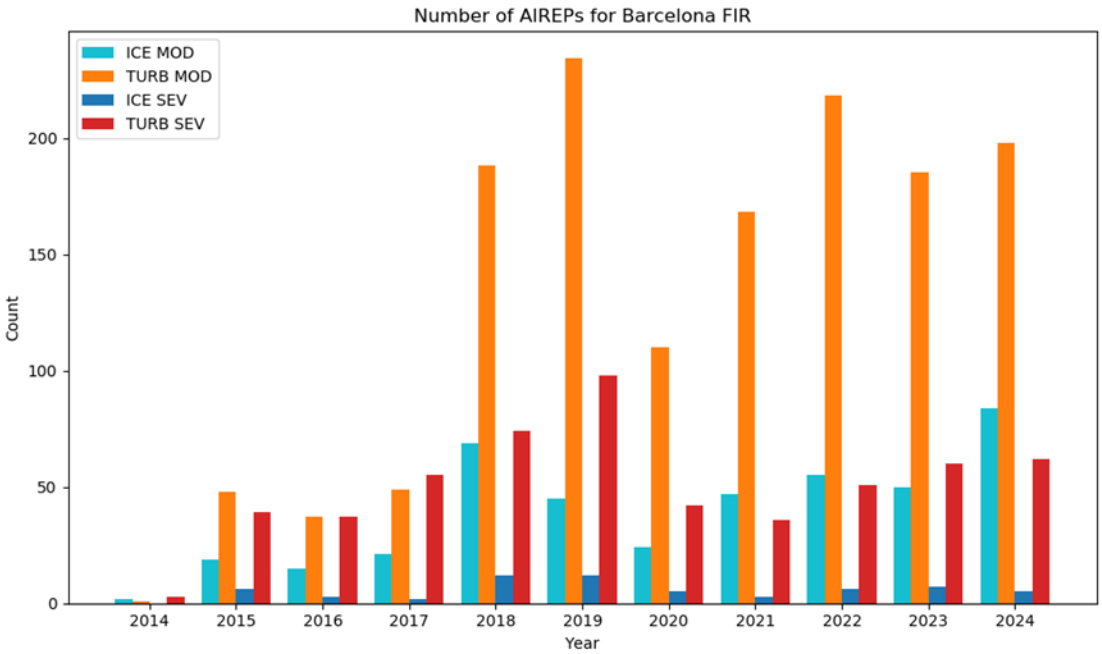

Figure 4. Annual number of AIREPs recorded within the Barcelona FIR during the 2014-2024 period.

With regard to moderate turbulence, an absolute maximum was recorded in 2019 with 234 reports, followed by a recovery during the post-pandemic period that led to 198 reports in 2024, with the 218 reports recorded in 2022 also standing out. In the case of severe turbulence, a similar pattern was observed, with a peak of 98 reports in 2019, followed by a decline and a partial recovery that resulted in a local maximum of 62 reports in 2024.

Moderate icing exhibited an upward trend following an initial peak in 2018 (69 reports), eventually reaching its absolute maximum in 2024 with 84 reports. Severe icing, meanwhile, recorded its highest values in 2018 and 2019, with 12 reports in each year, a level that has not been exceeded since.

The Canary Islands FIR exhibited substantially lower activity than the peninsular FIRs, with only 273 AIREPs recorded during the 2014-2024 period, representing just 5.2 % of the total dataset analysed (see Figure 5 and Table A-4). The COVID-19 pandemic did not have an appreciable impact on the reporting of observations in this region, largely due to the limited number of reports available prior to 2022.

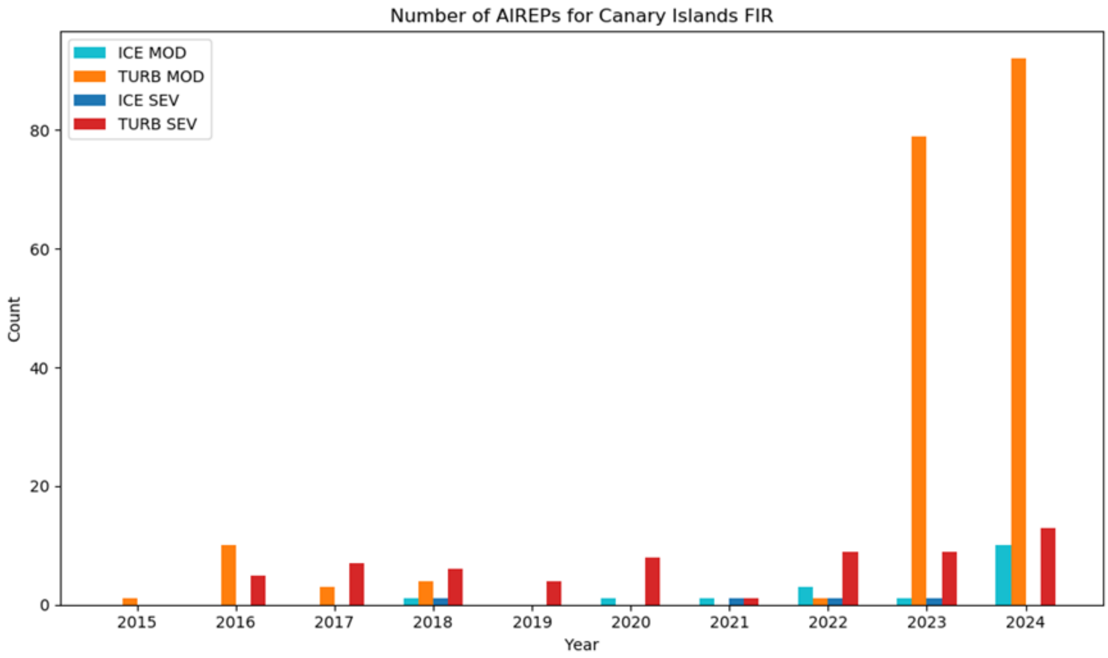

Figure 5. Annual number of AIREPs recorded within the Canary Islands FIR during the 2014-2024 period.

Regarding moderate turbulence, a pronounced increase is observed in the last two years of the study period, reaching a maximum in 2024 with 92 reports, followed by 79 reports in 2023. Moderate icing shows a very low frequency throughout the entire series, with a maximum of 10 cases in 2024 and isolated occurrences in 2018, 2020, 2021, 2022, and 2023.

Severe turbulence was first observed in 2016, reaching a maximum of 13 reports in 2024. Severe icing, on the other hand, was virtually absent, with only isolated cases recorded in 2018, 2021, 2022, and 2023.

3. MONTHLY ANALYSIS OF AIREP REPORTS IN SPANISH AIRSPACE

The monthly analysis of the AIREPs recorded across all Spanish FIR regions during the 2014-2024 period reveals a marked seasonality in the occurrence of significant meteorological phenomena, particularly with regard to turbulence and icing, as shown by the data presented in Figure 6 and Table A-5. This seasonality is reflected in a higher frequency of reports during the winter and transitional months, in contrast to the summer months, when activity decreases markedly.

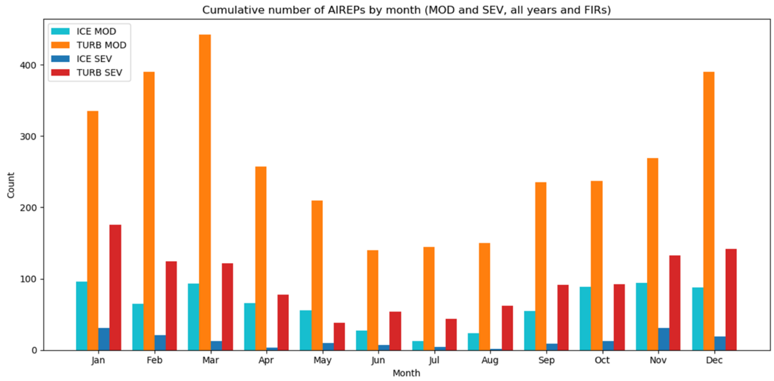

Figure 6. Monthly AIREP records for FIR Madrid, Barcelona and Canary Islands, period 2014-2024.

Moderate phenomena show a clearly winter distribution. March ranks as the most active month of the period, with a total of 535 moderate records, followed by December (478), February (455) and January (431). This concentration of reports coincides with the months of greatest atmospheric instability and conditions favourable for ice formation and turbulence generation.

Moderate turbulence is the most frequently reported phenomenon, with peaks in March (442 reports), February (390), December (390), and January (335). This pattern reflects the intensification of the jet streams and the increased occurrence of clear-air turbulence (CAT) during winter. Recent studies (Hermoso *et al.*, 2024) have shown that the jet stream is located at lower latitudes during the winter season, while the meridional temperature gradient (equator-to-pole) becomes stronger, leading to enhanced energy transport and, consequently, an increase in jet stream intensity. The relationship between CAT and jet stream wind maxima is well established, and as early as the mid-twentieth century it was linked to strong vertical wind shear near or within the jet stream (Clem, L.H., 1955). In addition, winter months are characterised by an increase in orographic turbulence and mountain waves, generated by the interaction between airflow and terrain under specific conditions of atmospheric stability and longitudinal vertical wind shear. Severe turbulence is the most frequently reported severe weather phenomenon, with maxima occurring in January (176 reports), December (142), November (133), February (124), and March (122). During the summer months (June, July, and August), activity decreases markedly due both to the northward displacement of the jet stream and to the lower frequency of atmospheric conditions conducive to mountain wave formation.

Moderate icing also exhibits a predominantly wintertime distribution, with peaks in January (96), March (93), October (89), November (94), and December (88). This pattern is consistent with the increased frontal activity characteristic of the cold season, which is associated with a greater prevalence of stratiform clouds containing supercooled liquid water droplets, conditions that favour icing formation. Empirical studies, such as those by (Fernández-González *et al.*, 2014) have demonstrated the relationship between icing occurrence and stratiform cloud systems. This relationship may be further enhanced by mesoscale orographic factors, such as the presence of a lee-side low or the generation of mountain waves beneath a temperature inversion located above the cloud layer. It should be noted that icing tends to be more severe within convective clouds; however, its spatial extent is generally more localised, and aircraft crews attempt to minimise exposure to these conditions whenever possible. Nevertheless, the presence of convective clouds may still contribute to the icing reports recorded during the summer season. Severe icing reaches its maximum frequency in January and November (31 reports each), followed by February (21), reflecting the greater prevalence of conditions favourable for aircraft structural icing during the cold season.

It is important to note that, although no definitive conclusions can be drawn regarding the annual evolution of AIREP reports in relation to variations in significant weather phenomena, since the primary driver of their increase was the progressive growth in air traffic volume, it is nevertheless possible to identify a clear seasonal relationship in the meteorological phenomena responsible for turbulence and icing conditions. This is evidenced by the fact that the monthly evolution of AIREP reports is inversely related to the number of flight operations.

These factors explain the concentration of AIREP reports during the colder months, which could suggest the need for enhanced meteorological surveillance during this period from an operational forecasting perspective. However, from the standpoint of aviation weather risk management, summer represents the season with the greatest impact over the Iberian Peninsula and the Balearic Islands, despite the statistics presented above. This is partly due to the increase in air traffic, particularly at airports located along the Mediterranean coast, and to the influence of convective activity. Table 2 shows the annual cycle of convective activity over the Iberian Peninsula and the Balearic Islands for the period 2007-2016, based on the lightning climatology developed and published by (Núñez *et al.*, 2019). The results reveal an increase in convective activity during the summer months, with a peak in September, which accounts for 23.9 % of the total annual lightning discharges.

Month	Jan	Feb	Mar	Apr	May	Jun	Jul	Aug	Sep	Oct	Nov	Dec
%	1.3	1.1	1.6	4.4	7.8	11.7	12.8	15.5	23.9	11.8	6.1	2.0

Table 2. Monthly percentage distribution of lightning discharges over the Iberian Peninsula and the Balearic Islands during the period 2007-2016.

In the case of the Canary Islands, unlike the Iberian Peninsula and the Balearic Islands, lightning activity does not exhibit a summer concentration but is instead distributed predominantly during the colder months. Table 3 presents the monthly distribution of lightning discharges over the Canary Islands for the period 2007-2016, based on the climatology developed by (Núñez *et al.*, 2019). Air traffic at Canary Islands airports shows a more homogeneous distribution throughout the year, associated with the milder climate of the archipelago and its status as a year-round tourist destination, as reflected in traffic statistics published by (AENA, 2025).

Month	Jan	Feb	Mar	Apr	May	Jun	Jul	Aug	Sep	Oct	Nov	Dec
%	7.2	12.2	11.1	0.5	0.8	0.2	0.4	4.4	2.2	13.2	31.7	16.1

Table 3. Monthly percentage distribution of lightning discharges over the Canary Islands during the period 2007-2016.

3.1 Monthly analysis by Flight Information Region (FIR/UIR)

The monthly evolution of AIREP reports within the Madrid FIR during the period 2014-2024 exhibits a marked seasonality, with a significant decrease in the number of reports during the summer months, particularly in July and August, as shown in Figure 7 and Table A-6. Given that this FIR accounts for approximately 47.8 % of the total AIREP reports analysed, its monthly behaviour is highly representative of the Spanish airspace as a whole.

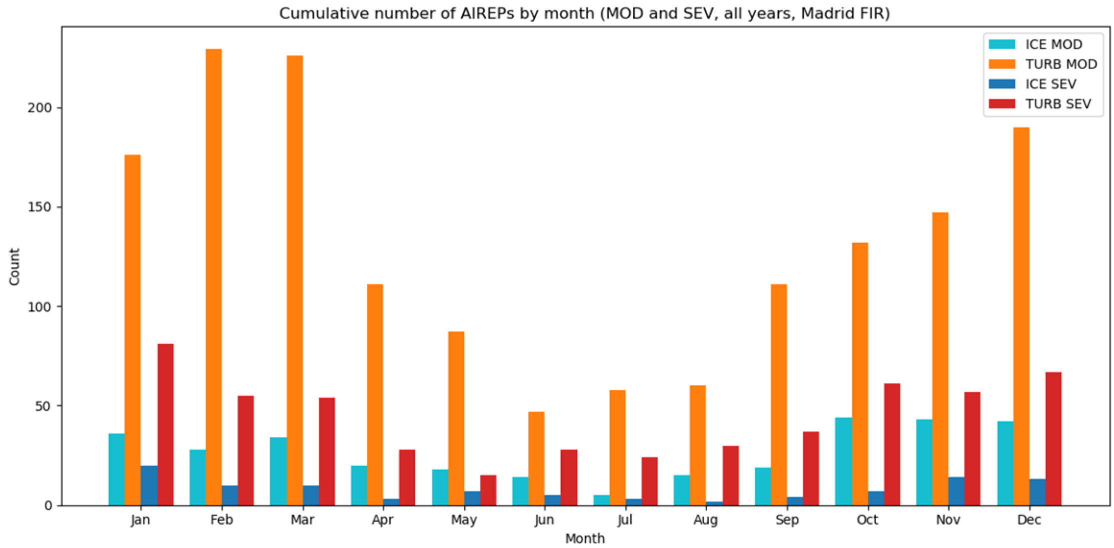

Figure 7. Monthly AIREPs distribution in the Madrid FIR region, 2014-2024.

Regarding moderate turbulence, a clear predominance is observed during the colder months, reaching a maximum in February with 229 reports.

Moderate icing, in turn, shows its highest incidence between October and January. This distribution is consistent with the onset of the cold season, when temperature and humidity conditions favour ice formation at flight levels.

As for severe phenomena, severe turbulence reaches its peak in January with 81 reports, remaining at relatively high levels throughout winter and autumn. Severe icing also records its highest frequency in January, with 20 reports, reinforcing the winter seasonality of this type of phenomenon and its potential impact on operational safety.

The monthly evolution of AIREPs in the Barcelona FIR during the 2014-2024 period exhibits a seasonal pattern similar to that observed in the Madrid FIR (see Figure 8 and Table A-7). A marked reduction in reports is observed during the summer months, particularly in July and August. This behaviour is associated with the lower occurrence of adverse meteorological phenomena, despite the increase in air traffic during the summer season.

Moderate turbulence reaches its maximum in March, with 192 reports, followed closely by December and January. Moderate icing, in turn, records its highest frequency in January, with 60 reports, coinciding with the most favourable conditions for in-flight ice formation.

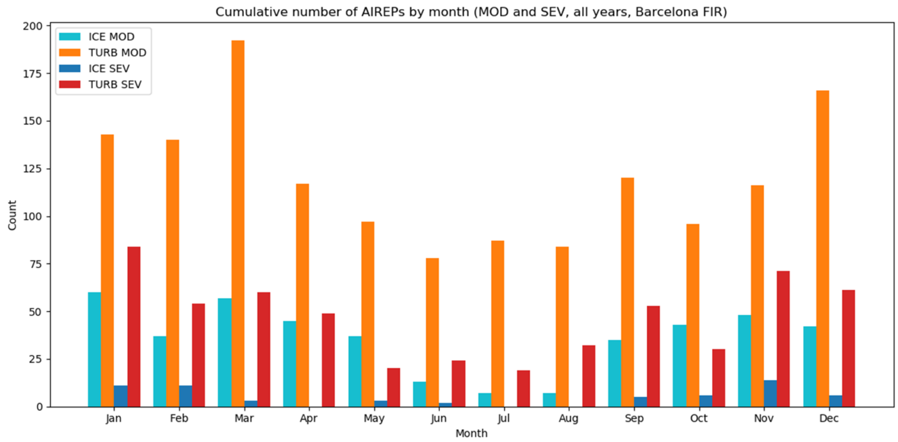

Figure 8. Monthly distribution of AIREPs in the Barcelona FIR region during the 2014-2024 period.

Regarding severe phenomena, severe turbulence peaks in January with 83 reports, remaining at elevated levels throughout November and December. Severe icing reaches its maximum in November, with 14 reports.

The monthly analysis of AIREPs in the Canary Islands FIR during the 2014-2024 period confirms the limited statistical representativeness of this region, which accounts for only 5.2 % of the total number of reports (see Figure 9 and Table A-8). This low data density prevents the identification of consistent monthly trends, although some isolated values can still be highlighted.

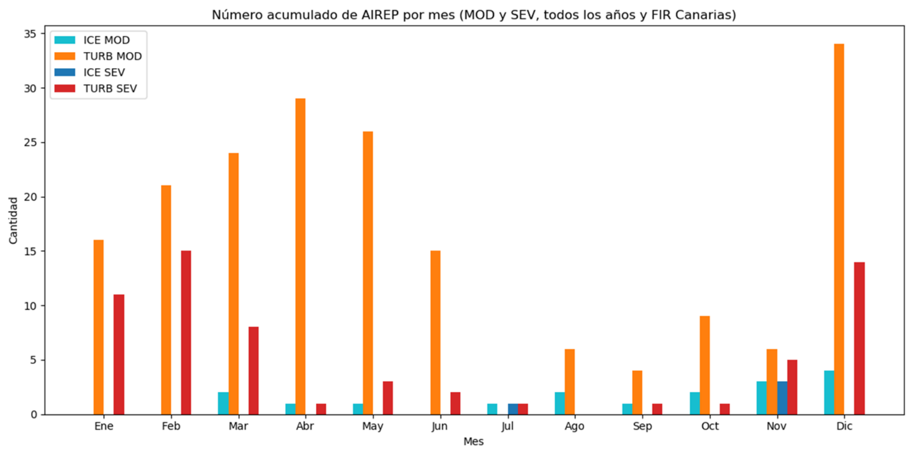

Figure 9. Monthly distribution of AIREPs in the Canary Islands FIR region during the 2014-2024 period.

Regarding moderate turbulence, the highest values are recorded during the winter and spring months, with December standing out with 34 reports, followed by April (29), May (26), and March (24). This pattern reflects higher activity during this period compared to the summer months, when values are considerably lower and even drop to zero in July. Moderate icing, in turn, shows a low frequency, with a maximum of 4 reports in December and isolated occurrences in the remaining months, being absent during several periods of the year.

Severe turbulence exhibits an irregular distribution, with a higher incidence in the winter months, particularly in February (15), December (14), and January (11), while in spring and summer the number of reports is much lower. As for severe icing, its occurrence is very limited, being recorded only in July (1 case) and November (3 cases), with no presence during the rest of the analysed period.

In the case of the Canary Islands, turbulence maxima are mainly associated with two factors. On the one hand, the intensification and approach of the subtropical jet, which occurs during the winter and spring months (E. Cuevas, 2001). The subtropical jet is generally less intense than the polar jet, and it typically generates moderate turbulence and, only in rare cases, severe turbulence. On the other hand, there are cut-off troughs descending from polar latitudes towards areas close to the archipelago, which eventually develop into cut-off lows and/or isolated cold lows in the vicinity of the islands. These situations are more frequent between November and January, although they can also occur in spring (Font Tullot, 1956). Due to the presence or proximity of an intense polar jet and its associated shear, as well as more organised and extensive convection, severe turbulence reports are more likely under these conditions.

The minimum observed during summer and early autumn is associated with the weakening of the subtropical jet during this time of year, and the absence of disturbances linked to the polar jet, which shifts significantly north of the archipelago.

4. MONTHLY ANALYSIS OF THE VERTICAL DESTRIBUTION OF AIREP REPORTS OVER SPANISH AIRSPACE

This section aims to characterise the monthly evolution of the altitudes associated with two meteorological phenomena of particular relevance to aviation: turbulence and icing. To this end, processed and visualized data corresponding to a complete year have been used. Out of a total of 5285 available records, 27 observations were excluded due to the absence of information in the flight level altitude fields. Consequently, the analysis was carried out on a refined dataset of 5258 valid records corresponding to the study period (2014-2024).

4.1 Turbulence

Figure 10 shows the monthly evolution of the vertical extent of turbulence reports. The shaded area corresponds to the interquartile range (IQR), which reflects the statistical dispersion between the first quartile (Q1, 25 % of the data) and the third quartile (Q3, 75 % of the data). In addition, the median for each month is represented by a continuous line, providing a central reference for the distribution.

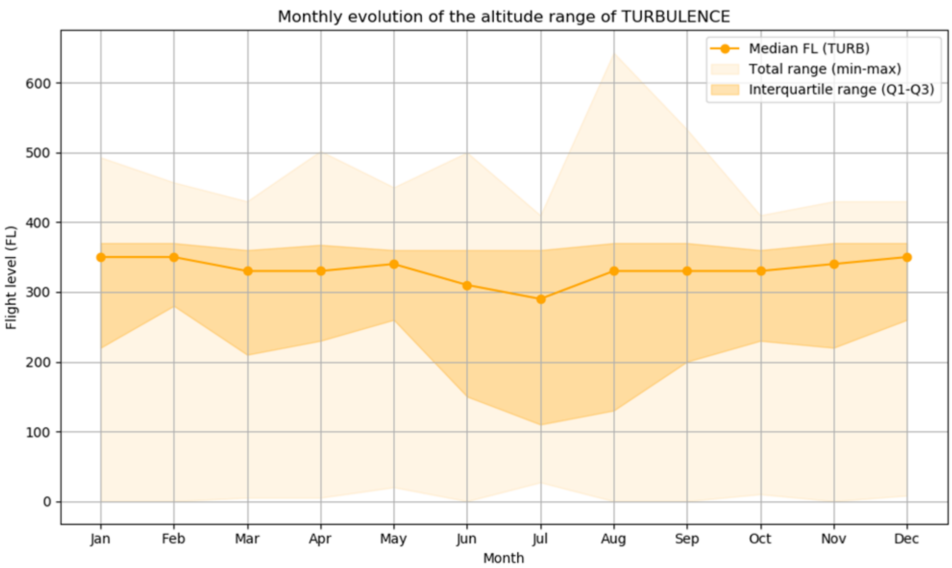

Figure 10. Monthly turbulence records at flight levels (FL) for the entire Spanish airspace, period 2014-2024.

The vast majority of turbulence events are concentrated between flight levels FL300 and FL390, especially during the colder months. This altitude band coincides with the typical height of polar jet streams. This is more clearly observed in Figure 11, where the monthly density of observations is represented as a function of altitude expressed in flight levels. During winter months, the circumpolar jet stream shifts to lower latitudes due to the stronger thermal gradient between the Arctic and mid-latitudes. As a result, the jet strengthens and is positioned further south, directly affecting the Iberian Peninsula and the Balearic Islands. This leads to a higher density of observations during the cold months within these flight levels, consistent with clear-air turbulence (CAT), which is very common near jet stream wind maxima.

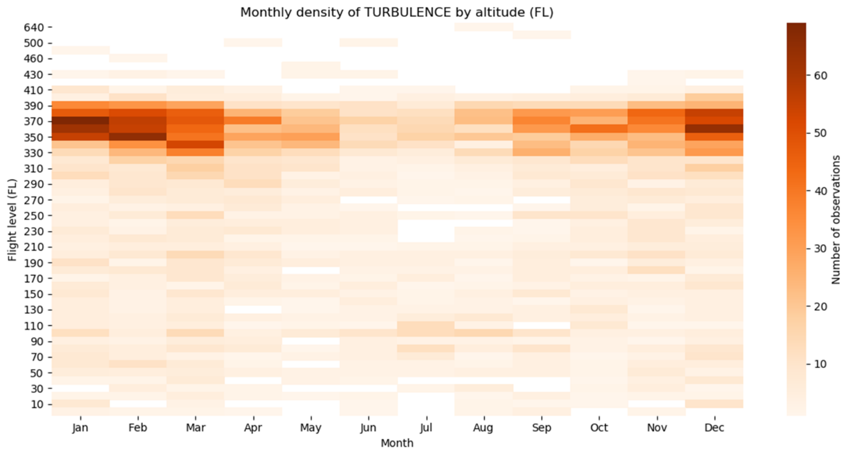

Figure 11. Monthly density of turbulence at flight levels (FL) for the entire Spanish airspace, period 2014-2024.

In contrast, during the summer months the jet stream is weaker and shifts northward, resulting in less CAT over Spanish airspace. Consequently, the number of observations decreases markedly, leading to the most significant events being distributed more homogeneously in the vertical, possibly because they are associated with convective developments or orographic turbulence.

The analysis of the monthly distribution of turbulence by flight level within the Madrid FIR reveals a clearly structured and consistent pattern throughout the year. The highest density of pilot reports is persistently concentrated in the upper troposphere, mainly between FL330 and FL390, where the core of maximum frequencies is located (see Figures 12 and 13, and Table A-10). This behaviour is further supported by the monthly evolution of the altitude range, with the median flight level of the reports remaining remarkably stable, fluctuating around FL340-360 throughout the year. Likewise, the IQR (Q1-Q3) remains relatively constrained within these levels, indicating low vertical dispersion among the most representative events.

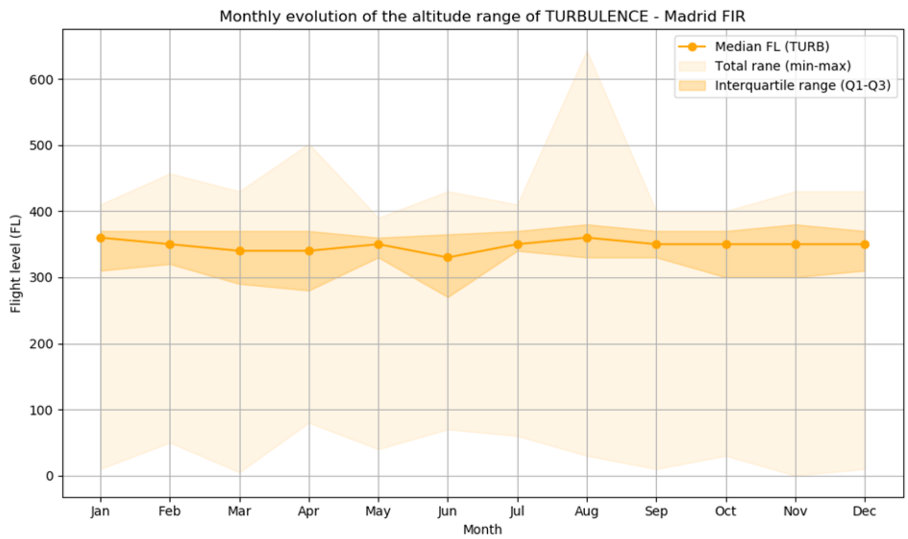

Figure 12. Monthly occurrence of turbulence at flight levels (FL) in the Madrid FIR region, period 2014-2024.

From a seasonal perspective, Figure 13 shows an intensification of the signal during the winter months (December to March), when the density of observations at higher flight levels increases, whereas during the summer months the activity decreases and becomes more dispersed. Nevertheless, even in summer, most reports remain concentrated at levels consistent with CAT.

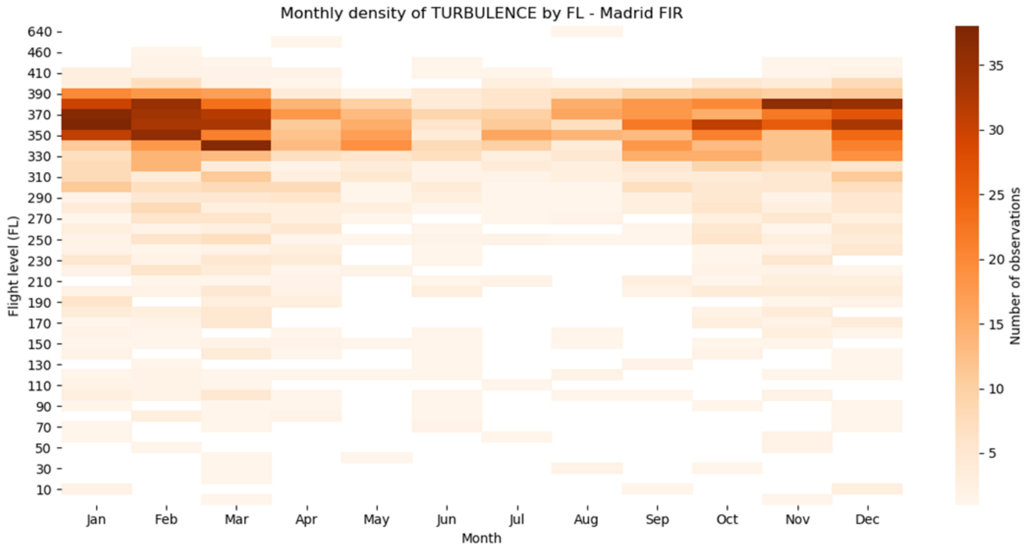

Figure 13. Monthly density of turbulence at flight levels (FL) in the Madrid FIR region, period 2014-2024.

In addition, a decrease in turbulence throughout the middle and lower troposphere is observed during the summer months, which could be related to a reduced contribution from orographically induced turbulence. At this time of year, the weaker synoptic-scale flows and the reduced occurrence of conditions favourable for the generation of mountain waves limit both the turbulence associated with wave breaking and the mechanical turbulence induced by the interaction of the wind with the terrain. Consequently, convective events become a more dominant mechanism as the contribution from dynamic and orographic processes decreases.

Overall, these results show that turbulence within the Madrid FIR exhibits a highly consistent vertical structure, dominated by large-scale dynamical processes associated with the jet stream and vertical wind shear, with only a limited contribution from local or convective mechanisms. This vertical homogeneity also suggests greater predictability of the phenomenon compared with other regions.

Regarding this latter point concerning the origin of turbulence, notable differences emerge when analysing the Barcelona FIR (Figures 14 and 15, and Table A-11) in comparison with the Madrid FIR. The interquartile range in the Barcelona FIR expands considerably, encompassing much of the middle and upper troposphere. This expansion is particularly pronounced during the summer months, when the median descends markedly towards mid-levels, in contrast to the more stable behaviour observed in the Madrid FIR. Therefore, there is a greater influence of processes that are not associated with the CAT generated by the jet streams linked to the polar front.

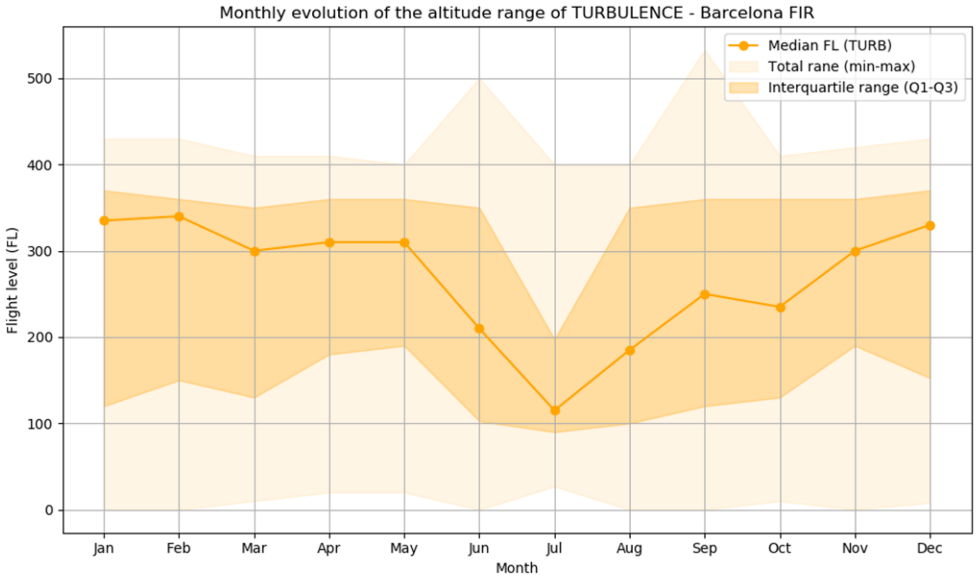

Figure 14. Monthly occurrence of turbulence at flight levels (FL) in the Barcelona FIR region, period 2014-2024.

This behaviour can be explained by the combined influence of several factors. First, the proximity to the Mediterranean Sea favours a greater supply of moisture and, consequently, a higher frequency of atmospheric instability situations, which translates into increased convective activity. This type of turbulence, which is more localised and vertically developed, contributes to broadening the range of affected altitudes.

Secondly, the interaction of the airflow with the complex topography of northeastern Spain, particularly in the vicinity of the Pyrenees and the Iberian System, favours the generation of orographic turbulence at different levels of the troposphere. Unlike the Madrid FIR, where the signal associated with the jet stream dominates, orographic mechanisms may play a more significant role in this region.

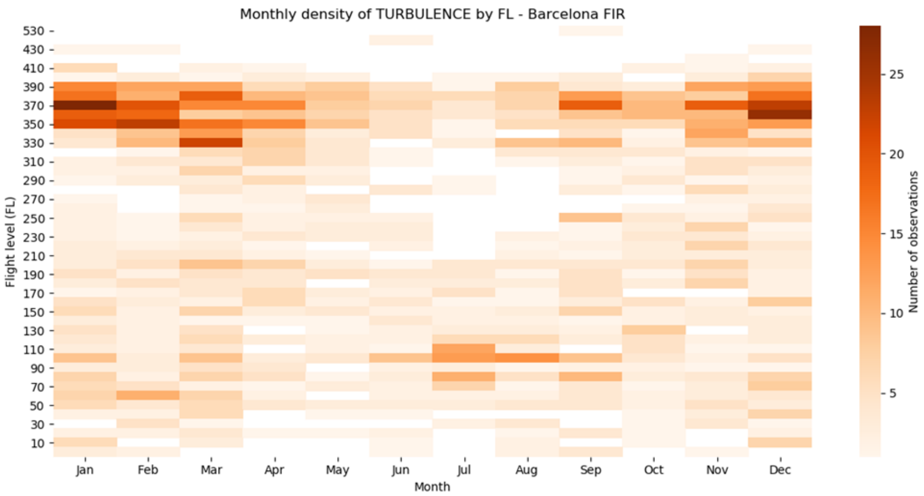

Figure 15. Monthly density of turbulence at flight levels (FL) in the Barcelona FIR region, period 2014-2024.

Thirdly, it can be considered that, under certain synoptic situations, the Barcelona FIR may be relatively more influenced by the subtropical jet stream than the Madrid FIR. In addition to the turbulence that the jet itself can generate through the associated wind shear, its presence may provide upper-level dynamical forcing, favouring the development of elevated convection over the Mediterranean region. This type of convection is associated with well-known meteorological situations and has been linked, among other phenomena, to the *rissagas* occurring in Ciutadella (Menorca) (Jansà *et al*., 2007). In this scenario, warm air advection from North Africa occurs around the 850 hPa level, leading to the formation of a very stable layer in the lower troposphere. As a consequence, convective triggering mechanisms become decoupled from the surface and develop above this inversion layer, within the middle troposphere where greater instability is present. This scenario may lead to the generation of turbulence at middle and upper levels, contributing to the widening of the interquartile range and to a greater vertical dispersion of pilot reports in the Barcelona FIR.

Figures 16 and 17 show the vertical distribution of turbulence pilot reports throughout the year within the Canary Islands FIR. It is noteworthy that the winter and spring months, which register the highest number of events, exhibit a regular behaviour with a relatively narrow interquartile range centred around flight level FL350. As discussed previously, this can be associated with the maximum intensity of the subtropical jet during this time of year, as well as with polar-origin disturbances extending southwards towards the islands.

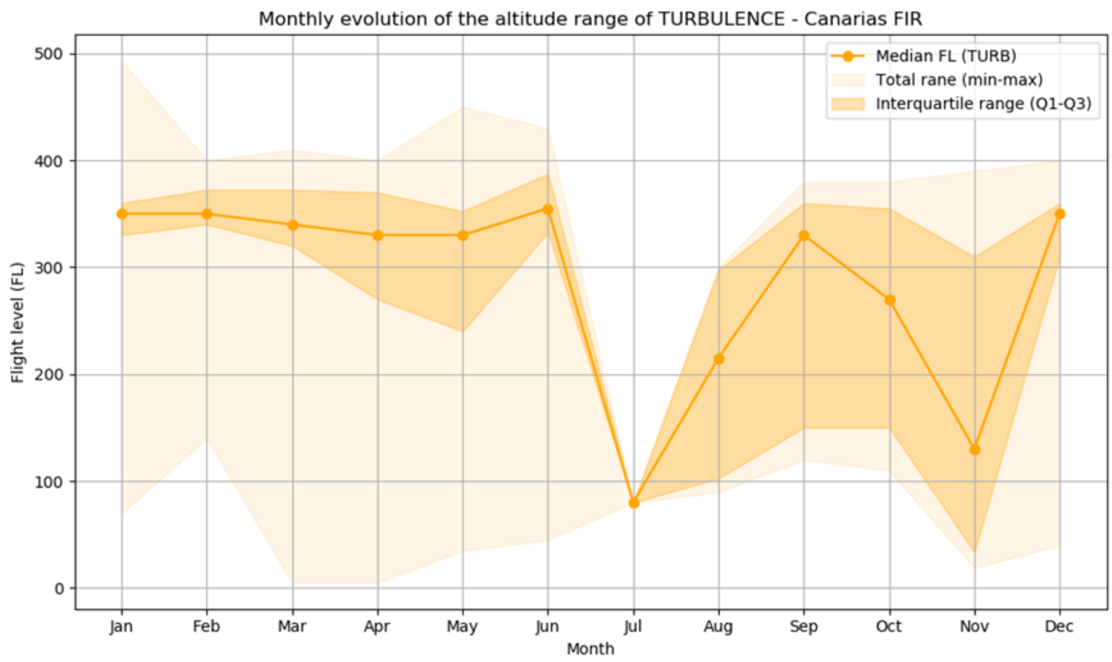

Figure 16. Monthly occurrence of turbulence at flight levels (FL) in the Canary Islands FIR region, period 2014-2024.

From June onwards, a change in the pattern becomes apparent. July stands out for the near absence of reports, while by late summer and early autumn the behaviour becomes more erratic, with a more heterogeneous distribution and a broader interquartile range extending from flight level FL100 to above FL300. The limited number of reports during these months does not allow firm conclusions to be drawn; however, it may reflect that this is the time of year when a wider variety of meteorological situations can occur. These months are the most favourable for the presence of easterly waves and disturbances of tropical and subtropical origin, in which dynamical forcing mechanisms are more commonly important in the lower and middle troposphere rather than in the upper troposphere. In addition, the first low-pressure systems of the winter half-year may begin to develop during this period.

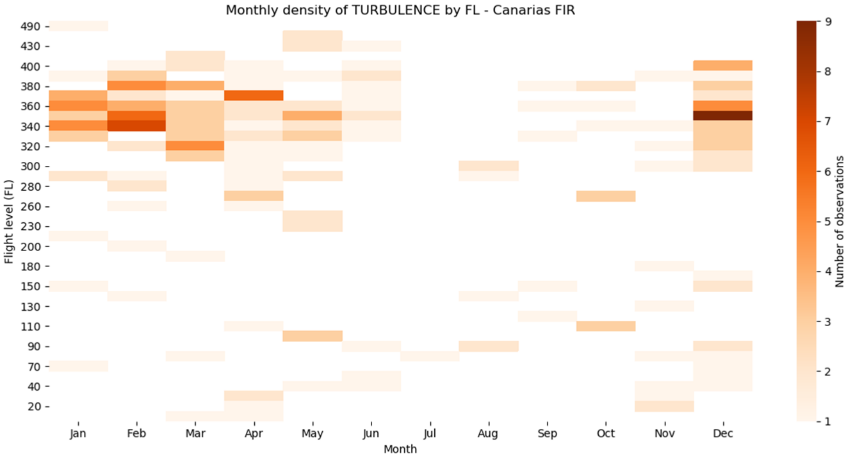

Figure 17. Monthly density of turbulence at flight levels (FL) in the Canary Islands FIR region, period 2014-2024.

4.2 Icing

Most icing cases are concentrated between FL100 and FL220, the range within which the interquartile range (Q1–Q3) is located for almost the entire year (see Figure 18 and Table A-13). Nevertheless, isolated events are observed both at very low levels (from FL010), due to intrusions of very cold air from northern latitudes during the winter season, and at altitudes above FL450. The latter are associated with convective processes, which allow icing to occur at lower temperatures than usual and, consequently, lead to observations being recorded at higher altitudes.

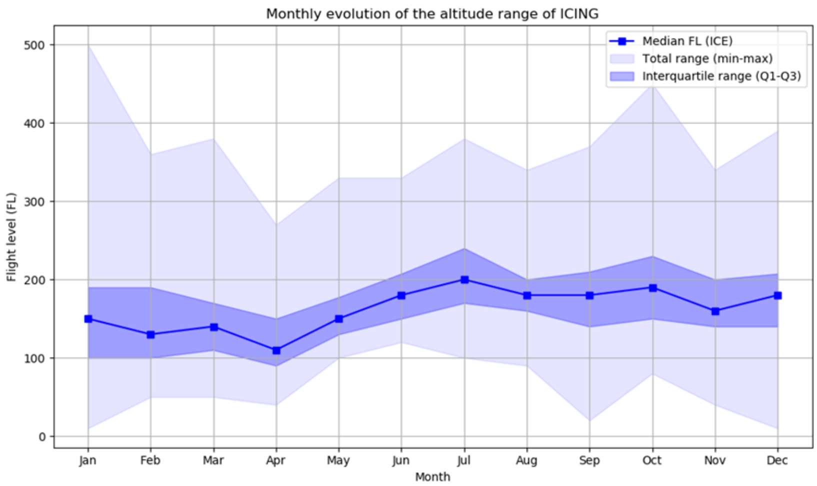

Figure 18. Monthly occurrence of icing at flight levels (FL) across the entire Spanish airspace, period 2014-2024.

It should be recalled that the temperature range in which icing is most efficient in stratiform conditions generally lies between 0 °C and –12 °C, reaching maximum efficiency between – 4 °C and –8 °C. This is the interval in which supercooled water droplets are most abundant and tend to be larger in size. Below –15 °C, icing efficiency decreases markedly, as most of the liquid water content within clouds tends to transform into ice crystals, thereby reducing the risk of ice accretion on aircraft.

However, in the case of convective clouds, the most severe icing may occur over a much broader temperature range, extending from the freezing level down to temperatures as low as – 40 °C. This is due to the presence of strong updraughts that transport liquid water from lower layers. These updraughts are capable of keeping large supercooled droplets (SLD) suspended, favouring a much broader vertical distribution of the phenomenon and allowing icing to occur at significantly higher altitudes than in stratiform situations. The droplets carried within the ascending currents eventually reach the cloud top, generally located near the tropopause, where they spread horizontally throughout the anvil and can extend far from the main convective core, often over distances of several tens of kilometres. Consequently, when an aircraft skirts a thunderstorm and enters the apparently harmless thin cirrus layer associated with the anvil, it may unexpectedly encounter icing conditions. It should also be emphasised that the severity and efficiency of icing depend not only on the environmental conditions but also on the duration of exposure to the phenomenon.

During the winter and spring months (January to April), icing tends to occur at lower flight levels, with the first quartile (Q1) generally located around FL080-100. This is consistent with the presence of a colder and more humid atmosphere in the lower and middle troposphere, where the development of supercooled stratiform clouds is favoured. These clouds are frequently associated with frontal surfaces, which are characteristic of the winter synoptic patterns affecting the Iberian Peninsula.

During the summer months (June to August), there is a significant decrease in the number of observations; however, the mean flight level affected by icing shifts upwards, reaching maximum values close to FL200-220. This behaviour is a consequence of the general increase in temperatures, which raises the freezing level to higher altitudes. Despite the reduction in frequency, the vertical extent of the affected layer remains broad, reflecting the altitudinal variability introduced by the convective processes typical of summer, in which icing is associated with more localised and dynamic cloud structures such as cumulus and cumulonimbus clouds.

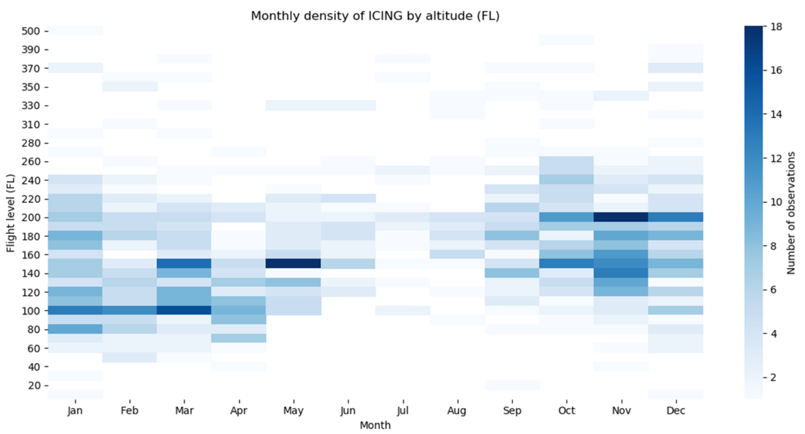

Figure 19. Monthly density of icing at flight levels (FL) across the entire Spanish airspace, period 2014-2024.

In summary, Figure 19 shows that icing exhibits a well-defined seasonal behaviour: in winter it dominates slightly lower layers and is linked to frontal systems and stratiform cloudiness, whereas in summer, although less frequent, it can occur at higher altitudes and is more associated with convection, while maintaining significant vertical dispersion.

The analysis of icing pilot reports in the Madrid FIR shows a clear seasonal modulation, both in frequency and vertical distribution. As shown in Figure 20 and Table A-14, the interquartile range (IQR) exhibits moderate variability throughout the year, with a shift in the distribution towards higher altitudes in summer, in line with the evolution of the tropospheric thermal structure. In contrast, the overall range (minimum–maximum) shows high variability in all months, with extremes that can extend from very low levels, around FL010 due to intrusions of very cold air, to altitudes close to FL400, particularly in more unstable atmospheric situations.

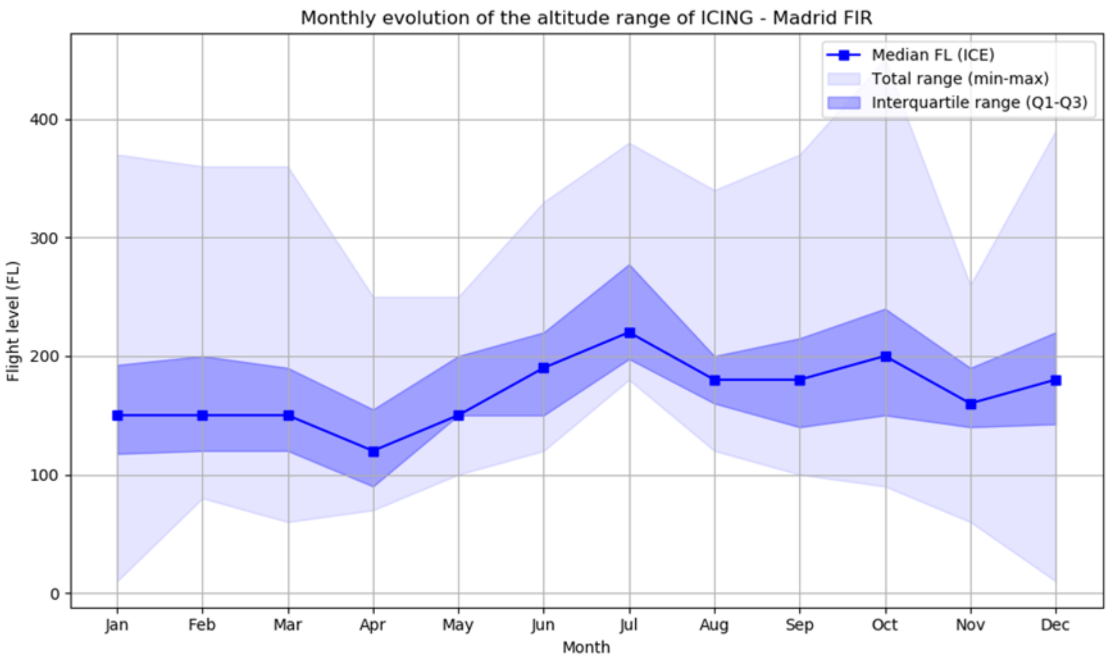

Figure 20. Monthly icing reports at flight levels (FL) in the Madrid FIR region, period 2014-2024.

In terms of density (Figure 21), icing is preferentially concentrated in the mid-levels of the troposphere, with a recurrent maximum between FL120 and FL200. The presence of icing at high levels (above FL300) is very limited and may be associated with convective events.

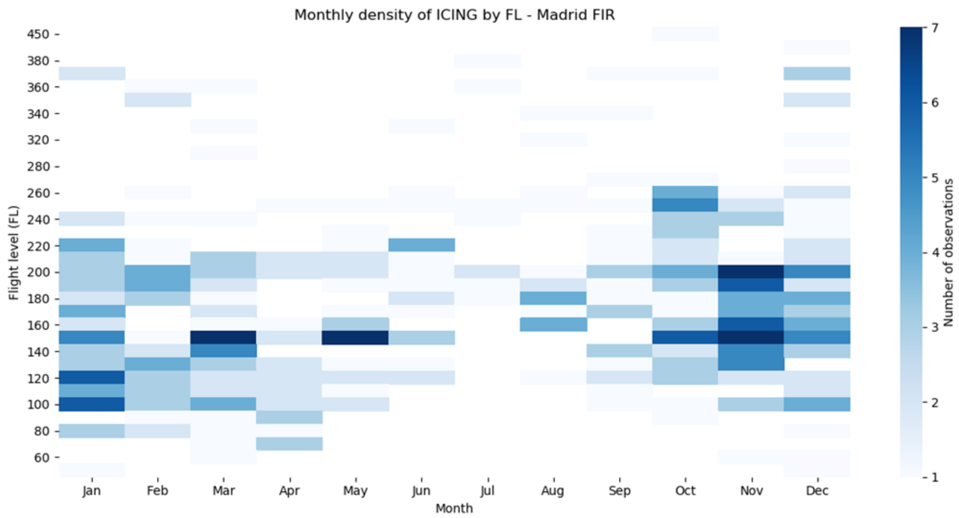

Figure 21. Monthly density of icing at flight levels (FL) in the Madrid FIR region, period 2014-2024.

In the Barcelona FIR (Figures 22 and 23, Table A-15), icing is observed to be mainly concentrated in both cases between flight levels FL100 and FL220, as was also the case in the Madrid FIR, a band that coincides with the typical atmospheric zone where supercooled clouds are present. However, differences are observed in the monthly evolution and in the vertical behaviour between both airspaces. In the Barcelona FIR, the vertical distribution of icing is more stable throughout the year, with a median that generally remains between FL140 and FL180. In contrast, in the Madrid FIR, the icing median is slightly higher for most of the year and shows a more pronounced monthly oscillation, with a clear upward shift during the summer months.

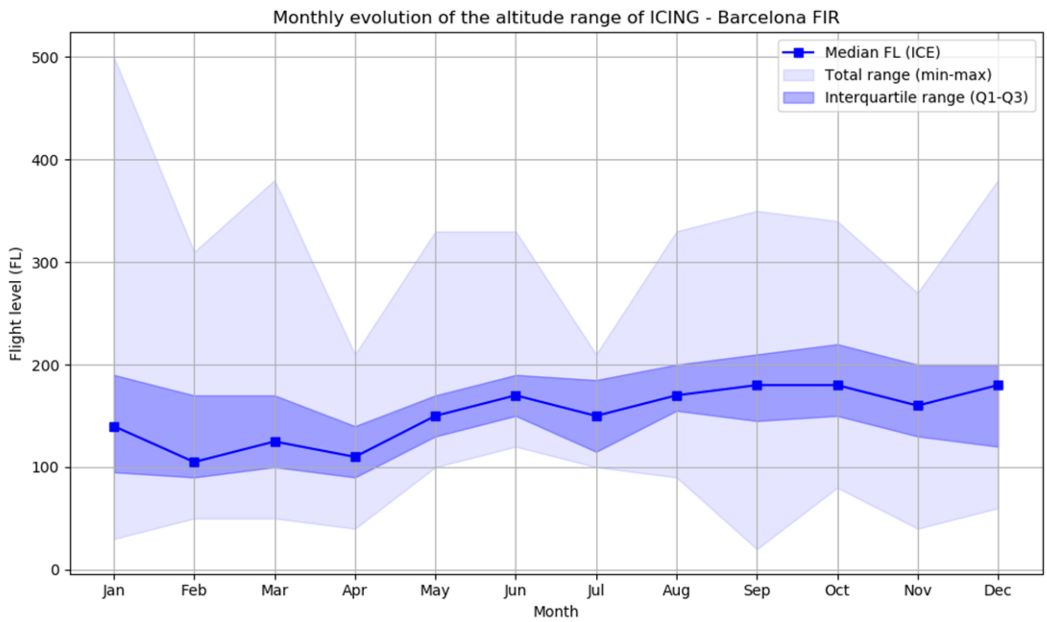

Figure 22. Monthly icing reports at flight levels (FL) in the Barcelona FIR region, period 2014-2024.

From a physical perspective, during the summer months in the Barcelona FIR, the proximity to the Mediterranean Sea favours the persistence of more humid profiles in the lower and middle levels of the atmosphere, leading to convective environments with cloud bases occurring at lower altitudes. In contrast, the higher summer elevation of the affected altitudes in the Madrid FIR can be associated with convective processes featuring higher cloud bases, typical of the inland Iberian Peninsula during summer, when the lower-tropospheric vertical profile is usually dominated by warm and dry air masses. Under these conditions, both the lifting condensation level and the freezing level rise, resulting in cumulonimbus cloud bases developing at higher altitudes and, consequently, icing phenomena being forced to occur in upper layers. For a more detailed understanding, the reader is referred to the concept of condensation levels (LCL and CCL) in the following module (UCAR/COMET, 2012).

Additionally, the Barcelona FIR shows, in several months, especially during autumn, a higher concentration of observations (Figure 23), which may be related to situations characterised by greater moisture content and atmospheric dynamism in the Mediterranean environment. In this context, intrusions of cold air aloft favour instability by interacting with a still relatively warm Mediterranean Sea, increasing latent heat and moisture fluxes from the surface and enhancing convective development. This mechanism contributes to the formation of environments conducive to supercooled liquid water in mid-levels and, therefore, to a higher likelihood of icing. Overall, these differences highlight the key role of thermodynamic factors and maritime influence in modulating the vertical distribution of icing between both regions.

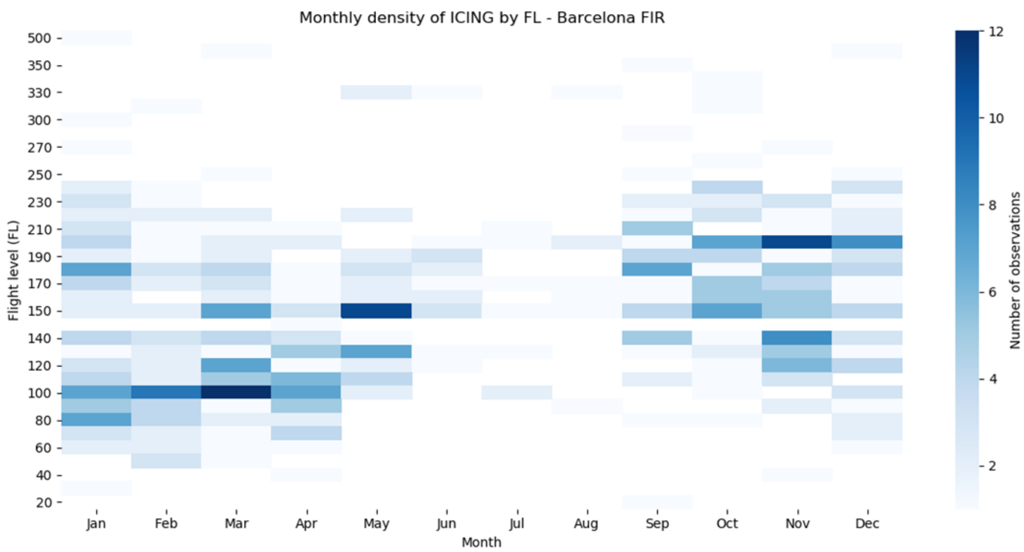

Figure 23. Monthly density of icing at flight levels (FL) in the Barcelona FIR region, period 2014-2024.

In contrast, the Barcelona FIR shows a more stable and moderate vertical profile, with the median altitude generally lower and a less pronounced seasonal variability (see Figure 22). Nevertheless, a slight decrease in mean altitudes is also observed during the colder months, consistent with a more humid atmosphere in the lower layers and conditions favourable for the formation of stratiform clouds with supercooled droplets. This also results in an increase in report density, clearly shown in Figure 23.

The scarcity of icing pilot reports in the Canary Islands FIR (see Figure 24 and Table A-16) can be explained by two factors. On the one hand, a strictly meteorological component associated with the predominance of a subsident and dry environment at the levels where this phenomenon typically occurs for much of the year, as well as the relative lack of synoptic disturbances capable of generating icing compared with the Madrid and Barcelona FIRs. On the other hand, the characteristics of the prevailing air traffic also play a role. Inter-island flights rarely exceed flight levels FL080–FL090, altitudes at which, even in winter, temperatures suitable for icing are very unlikely. Transoceanic flights connecting Europe and South America typically operate above FL330–FL360, where icing is also uncommon. Finally, flights connecting the islands with Europe do cross potentially favourable flight levels in a limited layer, where most of the few icing reports are typically located.

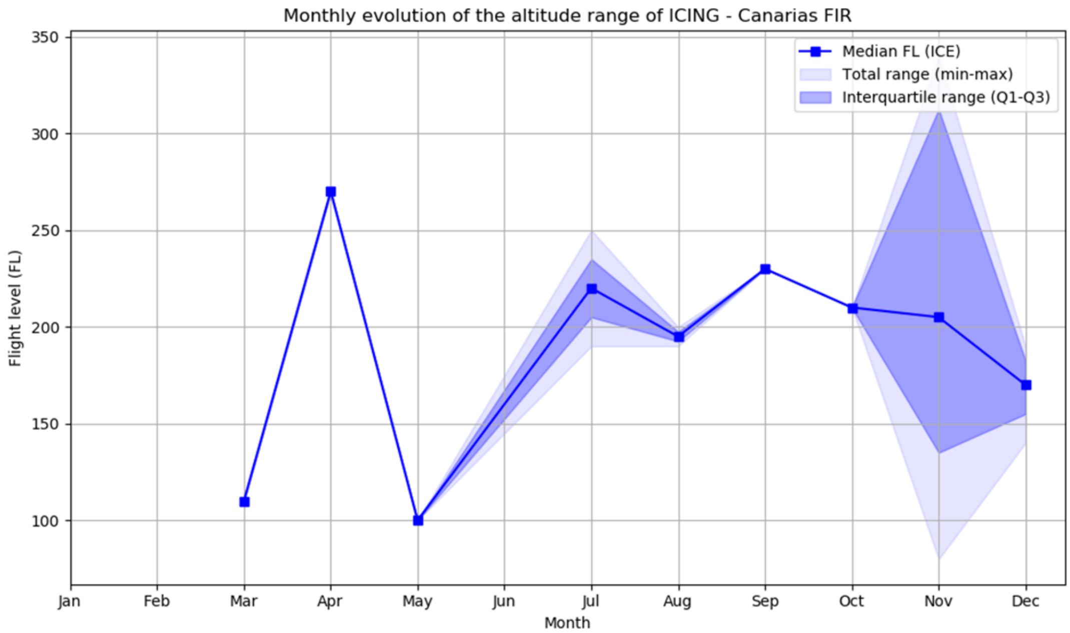

Figure 24. Monthly icing reports at flight levels (FL) in the Canary Islands FIR region, period 2014-2024.

Figure 25 reinforces this interpretation, showing a very limited and episodic occurrence of the phenomenon, with a complete absence of reports in several months of the year. Observations are very scarce and are distributed between flight levels FL080 and FL340. In addition to the reasons previously discussed, this marked scarcity of observations suggests the need to make their reporting more efficient and more automated, in order to ensure that they are reported in real time and inserted into the database.

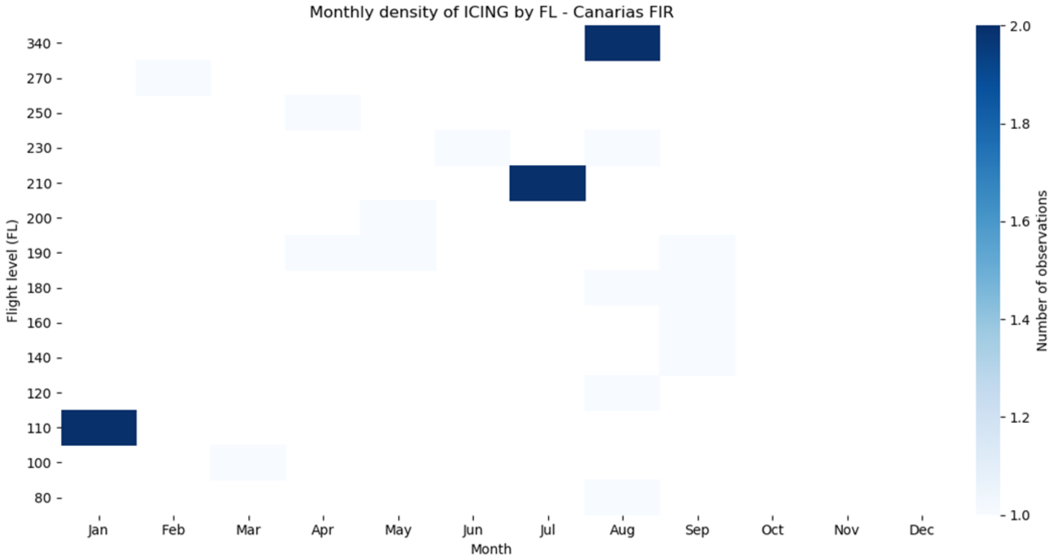

Figure 25. Monthly density of icing at flight levels (FL) in the Canary Islands FIR region, period 2014-2024.

5. TURBULENCE AND MOUNTAIN WAVES IN THE MAIN OROGRAPHIC SYSTEMS OF THE IBERIAN PENINSULA

In addition to turbulence associated with upper-level jets or mechanical turbulence generated at low levels by the purely mechanical interaction of the flow with orography, there is another relevant phenomenon in mountainous environments: mountain waves. These form when a stable air mass is forced to rise upon encountering an orographic barrier. Under certain atmospheric stability conditions (temperature and humidity profiles) and wind shear (vertical changes in speed and/or direction), this forced ascent can generate stationary waves that propagate both vertically and horizontally downstream of the mountain range; for more detail, a reading of the course (UCAR/COMET, 2014) is recommended.

If these waves encounter a favourable environment, such as stable stratification above a layer of strong shear or a temperature inversion, they can amplify vertically. In certain situations, these waves reach such amplitude that they become dynamically unstable, leading to wave breaking, analogous to how an ocean wave breaks. This breaking generates regions of intense turbulence that can extend from low levels up to the tropopause and even penetrate into the lower stratosphere. (Clark and Peltier, 1977) suggest that when isentropic lines in a mountain wave overturn, a resonant cavity forms between the terrain and the breaking region; all of this occurs under critical conditions where the Richardson number is less than 0.25 (Clark and Peltier, 1983).

In theory, this type of phenomenon should be specifically identified in AIREP reports using the label ‘MTW’ (Mountain Wave). However, in practice, the identification of the source of turbulence is subject to the subjective interpretation of the reporting pilot. As a result, it is common for turbulence episodes generated by mountain waves to be recorded simply as ‘TURB’, without distinguishing the underlying physical mechanism. In addition, it may occur that episodes labelled as ‘MTW’ are actually associated with turbulence of a different origin.

Therefore, if a more specific analysis of each event is desired, it would be necessary to examine the atmospheric conditions prevailing at the time of the report, such as the vertical stability profile, wind direction and intensity, and the relative position with respect to mountain systems, or simply verify whether cirrostratus clouds (Cs) have formed on the leeward side of the mountain range in satellite imagery from WV6.2, WV7.3, or even IR10.8 channels, in order to properly discriminate whether a report labelled as TURB may in fact be due to a mountain wave that has broken vertically.

This section presents the annual and monthly evolution of the number of turbulence (TURB) and mountain wave (MTW) reports associated with the main mountain systems of the Iberian Peninsula. This analysis provides a global view of the seasonal behaviour of these phenomena and their reporting frequency in the most significant orographic regions.

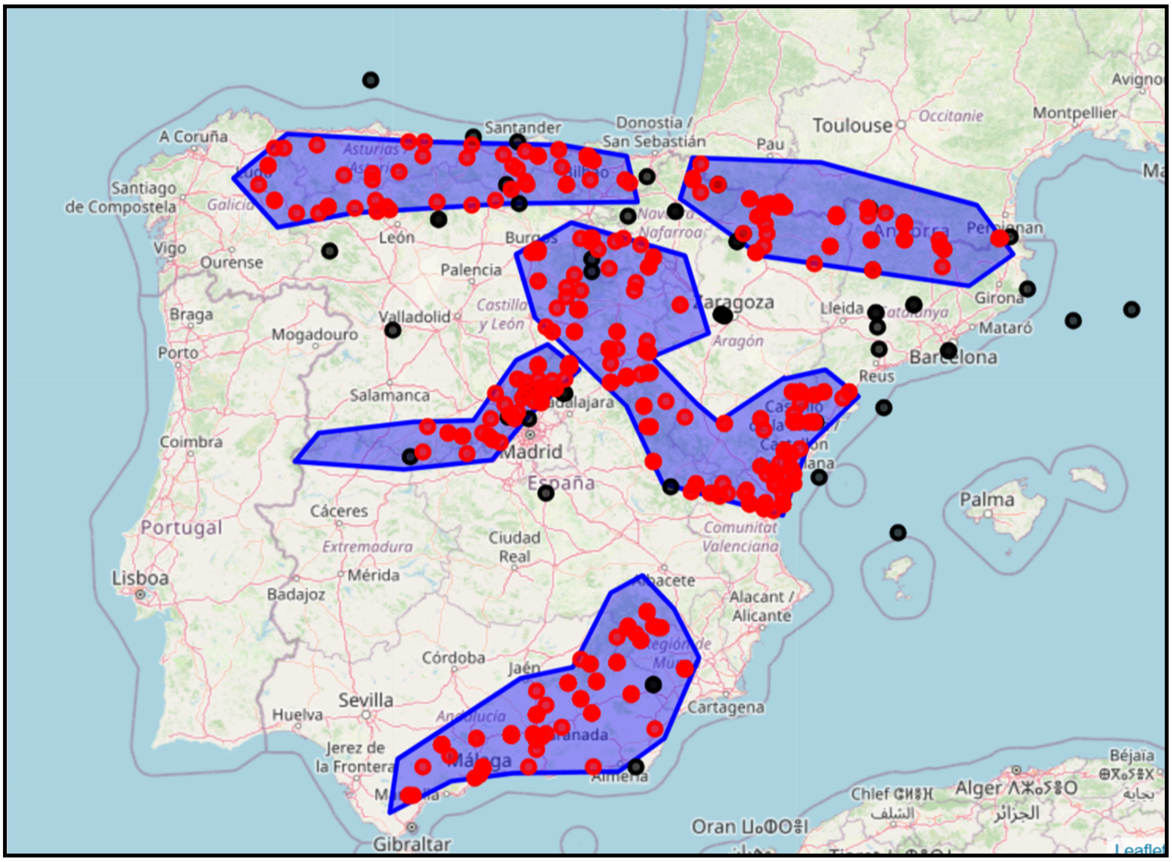

Figure 26. Distribution of AIREP mountain wave reports (in black) in the Madrid and Barcelona FIRs, and turbulence reports (in red) over the main orographic systems of the Iberian Peninsula, period 2014-2024.

Figure 26 shows, in black, the observations identified as mountain waves, highlighting their very low frequency over the study period. In red, turbulence reports located within the main mountain systems are represented, allowing their possible relationship with orography to be visualized. It is noteworthy that there are no recorded mountain wave observations for the Canary Islands FIR.

When interpreting aircraft reports, it is important to remember that their recording does not depend solely on the actual frequency of the physical phenomenon generating the turbulence, regardless of its origin or mechanism. It is also influenced by operational and human factors, such as the volume of air traffic crossing each mountain system, the pilot's proactiveness in issuing the report, and the actions of the ACC Watch Manager responsible for its handling and dissemination. Likewise, the possible introduction of human errors during the transmission of the aircraft report from AEMET's MWO should not be ruled out.

If the annual evolution of AIREP reports in the main mountain systems of the Iberian Peninsula is analysed, breaking down TURB and MTW phenomena by intensity (moderate and severe), a clear predominance of turbulence reports over mountain wave reports is observed, see Figure 27 and Table A-17.

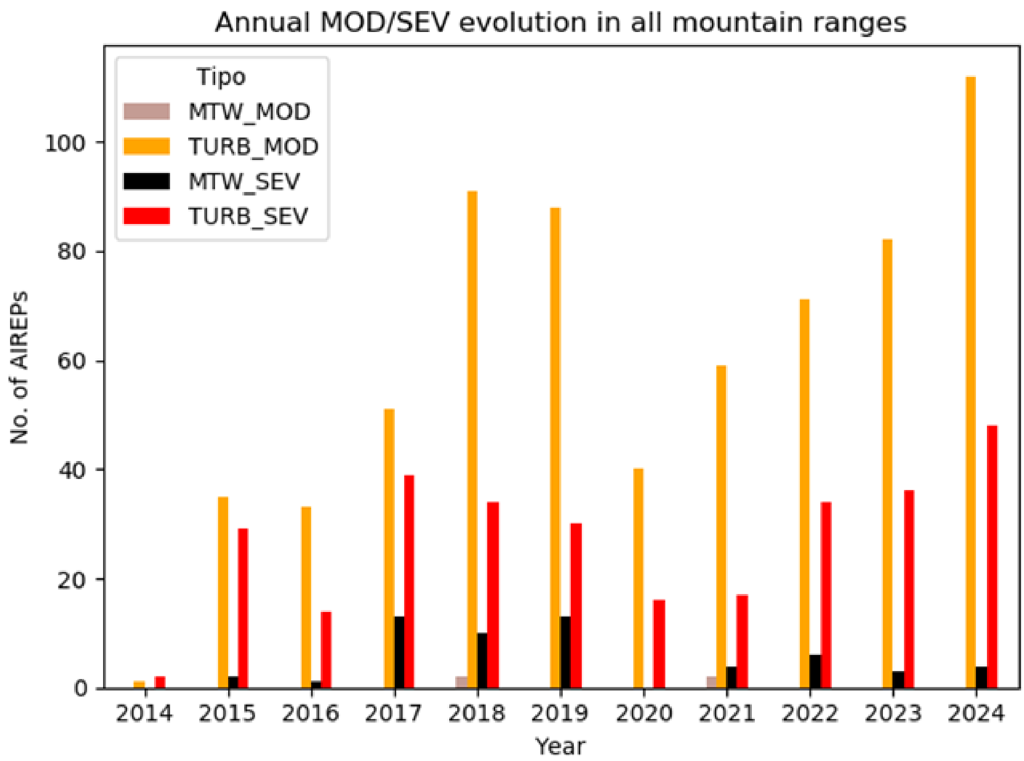

Figure 27. Annual AIREP record of turbulence and mountain wave for all mountain systems, period 2014-2024.

In particular, moderate turbulence reports show an increasing trend since 2014, with a notable decrease in 2020 due to the impact of the COVID-19 pandemic, followed by a sustained recovery reaching a maximum in 2024. Severe turbulence follows a similar pattern, although with a lower total volume.

On the other hand, mountain wave reports are significantly scarcer. It is striking that severe mountain wave cases outnumber those of moderate intensity, which could be due to a greater ease of identification or reporting of more intense events. These moderate MTW reports appear sporadically in 2018 and 2021, with only two records in each year.

The monthly analysis of AIREP reports shows a clear predominance of turbulence and mountain wave notifications during the winter months, especially between December and March, see Figure 28 and Table A-18. This seasonal distribution is consistent with the atmospheric dynamics discussed in previous sections, according to which, during cold seasons in mid-latitudes, jet streams at mid and upper levels shift equatorward and tend to intensify due to the stronger meridional thermal gradient characteristic of these regions. Under these conditions, when upper-level confluence prevails (upstream of a trough or downstream of a ridge), subsidence creates the appropriate stability conditions over orographic systems, and upper-level jets provide sufficient longitudinal shear that allows mountain waves to break vertically. As previously noted, reports explicitly labelled as "MTW" are scarce; it is likely that many of these events are coded as "TURB" due to the inherent subjectivity in pilots' perception of the phenomenon. Despite this limitation, the pattern observed in the data reflects a clear increase in moderate and severe turbulence in the winter months, suggesting a significant influence of mountain waves, although their origin may also be different.

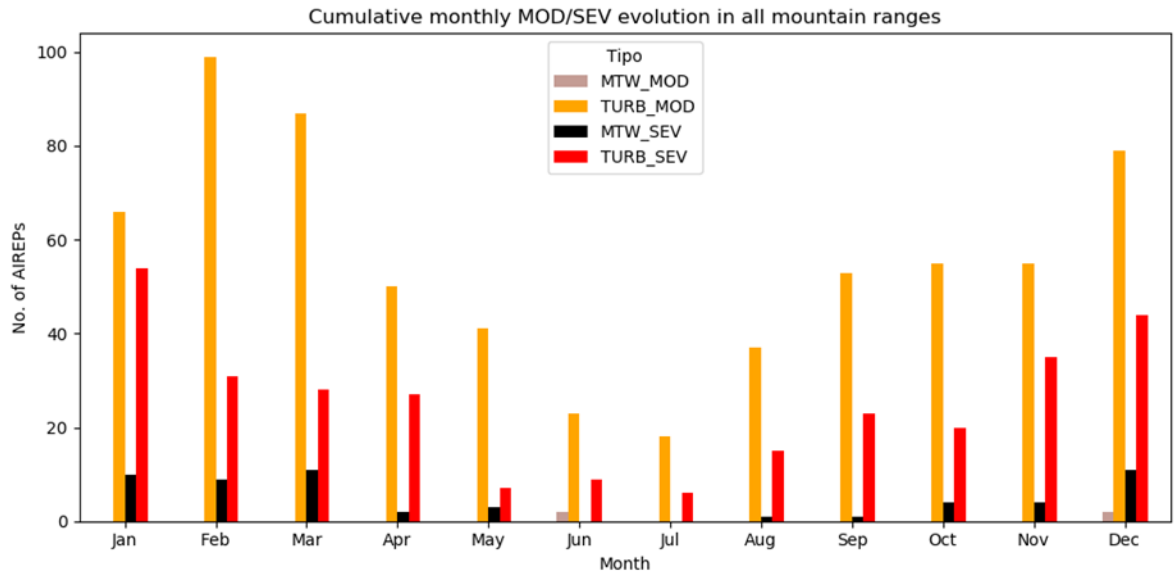

Figure 28. Monthly accumulated AIREP record of turbulence and mountain wave for all mountain systems, period 2014-2024.

On the contrary, during the summer months, especially between June and August, the number of turbulence reports decreases notably. At this time of year, thermal convection is a more common mechanism for generating turbulence, but its localised nature and its development in narrow, transient vertical columns mean that it does not always coincide with aircraft flight paths or can be easily avoided in flight. In addition, convection generates a type of turbulence that is different from orographic turbulence, generally less spatially extensive and more dependent on diurnal evolution. All of this contributes to the fact that the total number of AIREP reports in mountainous areas is considerably lower during the summer.

The monthly distribution of reports shows fairly marked seasonal patterns:

Turbulence is the most reported phenomenon throughout the year, but with peak values in the winter months. Peaks of moderate turbulence are observed in February (99), March (87), and December (79), while severe turbulence shows its highest incidence in January (54) and December (44).

Severe mountain wave activity has a more sporadic presence, with maxima in March (11) and December (11), while moderate cases are practically non-existent, except in June and December, with only 2 reports in each. Although less frequent, these events also tend to be concentrated in the cold months.

5.1 The Pyrenees

The geographic polygon defined for the Pyrenees mountain range has a perimeter of 863 km and covers an area of 34 184 km². For favourable conditions to develop that allow the formation and subsequent breaking of mountain waves with vertical propagation, it is essential that upper-level jet streams acquire a marked meridional component. This configuration favours air flow crossing perpendicularly to the mountain range's main axis, which is the optimal condition for the formation of well-developed orographic waves, as observed in (EUMETSAT, 2004) for the Iberian Peninsula and the Balearic Islands. It is in situations of northerly flow when the generated waves can break on the lee side, leading to significant turbulence in Spanish airspace. In some high-severity cases, this turbulence can even manifest as a dry band that appears dark in water vapour satellite imagery, associated with strong downdrafts and abrupt altitude variations.

It should be noted that turbulence is not always associated with the breaking of mountain waves. The simple mechanical interaction between the airflow and the Pyrenean terrain can also generate significant turbulence. Given that much of the mountain range reaches altitudes above 3000 metres, it facilitates the upward propagation of turbulence generated into the mid-troposphere. Notable examples of these high peaks include Aneto (3404 m), Posets (3368 m), and Monte Perdido (3355 m). In addition, turbulence at mid and upper levels may be recorded in association with jet stream wind maxima, even in the absence of direct interaction with orography, which further highlights the complexity of the turbulent environment over this region.

The area representing the Pyrenees shows the highest percentage of severity compared to other orographic systems, at 62.4 %. Moreover, a significant level of activity has been reported in absolute terms (221 records). This behaviour is consistent with its complex orography and its interaction with the atmospheric flows described above, making it the most critical region in terms of operational impact.

In the case of the Pyrenees, convective activity constitutes a relevant factor in the generation of turbulence, especially during the warm months. According to the climatology of lightning discharges in Spain (Núñez *et al*., 2019), this mountain range exhibits a high density of lightning strikes in summer, with more pronounced maxima in its eastern sector. This behaviour is related to the interaction between orographic forcing and the influence of the Mediterranean, which provides moisture and favours the development of deep convection. The Pyrenean topography acts as an effective convective trigger mechanism, leading to thunderstorms that can reach significant vertical development. The associated convection contributes to the generation of turbulence at mid and upper levels through intense updrafts, downdrafts, and shear zones. This may explain the recurrence of turbulence aircraft reports during the summer period in this region, especially in the eastern Pyrenees, complementing episodes associated with mountain waves.

The annual evolution of AIREP reports, as shown in Figure 29 and Table A-19, exhibits notable variability in the frequency of both turbulence and mountain waves. It is observed that the years with the highest activity, such as 2018, 2022, and 2024, record significant peaks in moderate and severe turbulence. A decrease is observed in 2020 and 2021, which is associated with the reduction in flights as a consequence of COVID-19.

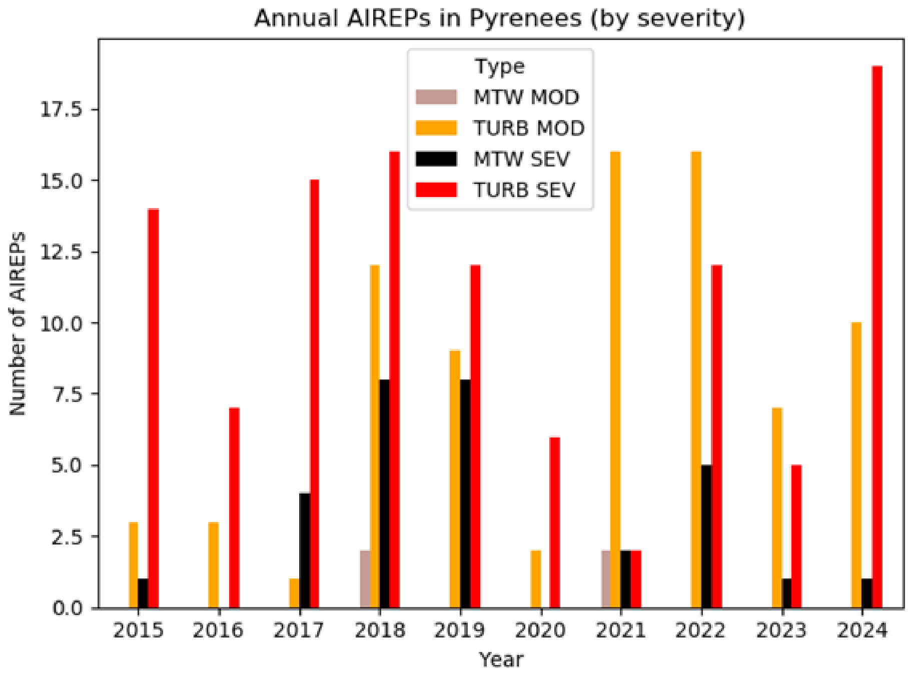

Figure 29. AIREP records of turbulence and mountain wave in the Pyrenees, period 2014-2024.

The monthly analysis shown in Figure 30 and Table A-20 confirms that the winter months concentrate the highest turbulence activity, with January, February, and December standing out, where elevated values of severe turbulence and severe mountain waves are recorded.

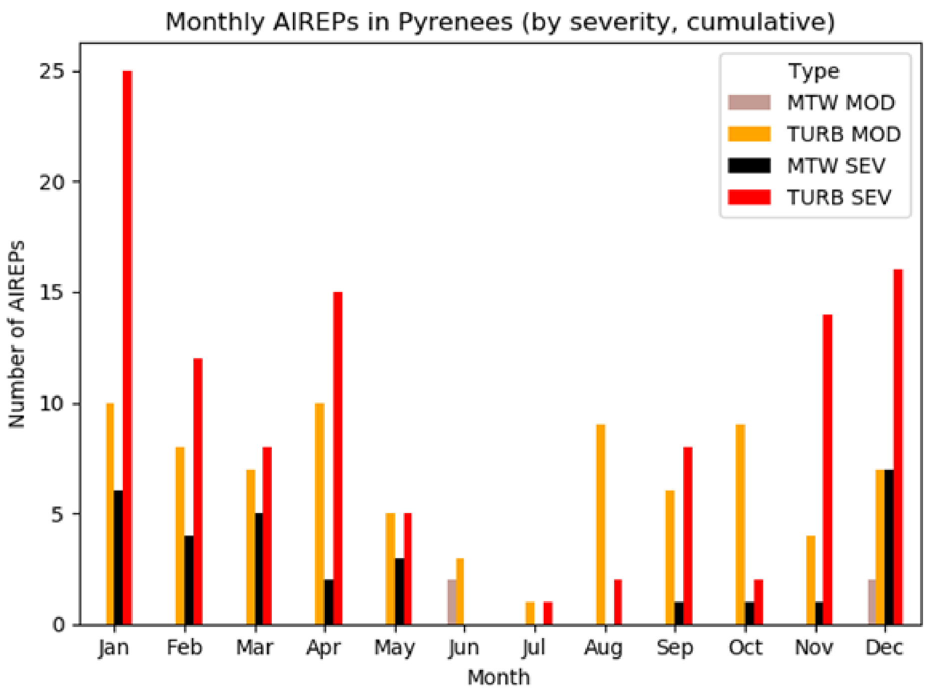

Figure 30. Monthly accumulated AIREP records of mountain waves and turbulence in the Pyrenees, period 2014-2024.

5.2 The Cantabrian Range

The geographic polygon defined for the Cantabrian mountain range has a perimeter of 1002 km and covers an area of 32 244 km². For a wind configuration coming from the NW quadrant, mountain waves trapped horizontally in the Cantabrian range and other mountain systems can often be observed; an example of this is a study conducted by (Díaz-Fernández *et al*., 2022). Another favourable atmospheric configuration for the generation of mountain waves occurs when the mountain range is located in the warm sector of a baroclinic cyclone. In this context, a stable layer is sometimes established above the mountain peaks, which is a necessary condition for the development of orographic waves. The presence of southwesterly (*ábregos*) winds, which impinge with some perpendicularity on the range from the northern plateau, favours the amplification and eventual breaking of these waves at upper levels. Once the cold front approaches, the atmosphere begins to destabilise from the surface upward and the southwesterly flow tends to veer toward the northwest, ending the possibility of continued mountain wave activity.

As in the previous case, mechanical interaction between the airflow and the orography can also generate dynamically induced turbulence that reaches mid-tropospheric levels. This phenomenon is particularly relevant in border areas of León, Asturias, and Cantabria, where numerous peaks exceed 2500 metres in altitude, such as Torre Cerredo (2650 m), Torre Blanca (2619 m), and Peña Vieja (2616 m). Given its northern location within the Iberian Peninsula, this region has a higher probability, compared to other mountain systems, of experiencing turbulence at mid and upper levels associated with jet stream wind maxima.

The contribution of convective activity to turbulence generation is generally limited. According to lightning climatology (Núñez *et al*., 2019), this region exhibits a relatively low density of lightning compared to other areas of the Iberian Peninsula, suggesting a lesser development of deep convection. Consequently, turbulence observed in this system is more frequently associated with Flow-terrain interaction and larger-scale dynamical processes than with convective phenomena.

The selected area representing the Cantabrian range shows low total activity, but a relatively high severity percentage (40.8 %). This indicates that, although fewer events are recorded, when they do occur they tend to present higher intensity, which may have relevant implications for air traffic management.

Between 2015 and 2024, as shown in Figure 31 and Table A-21, most of the reports recorded in the Cantabrian mountain range correspond to moderate turbulence, with an overall increase in the second half of the period analysed, highlighting the years 2017 (7 cases) and 2022 (8 cases). Severe turbulence has also been reported more frequently since 2017, reaching a maximum of 8 reports in that same year. Regarding mountain waves, reports have been scarce, especially in their moderate category, with a complete absence throughout the entire period. Only two cases of severe mountain waves were recorded, in the years 2019 and 2024.

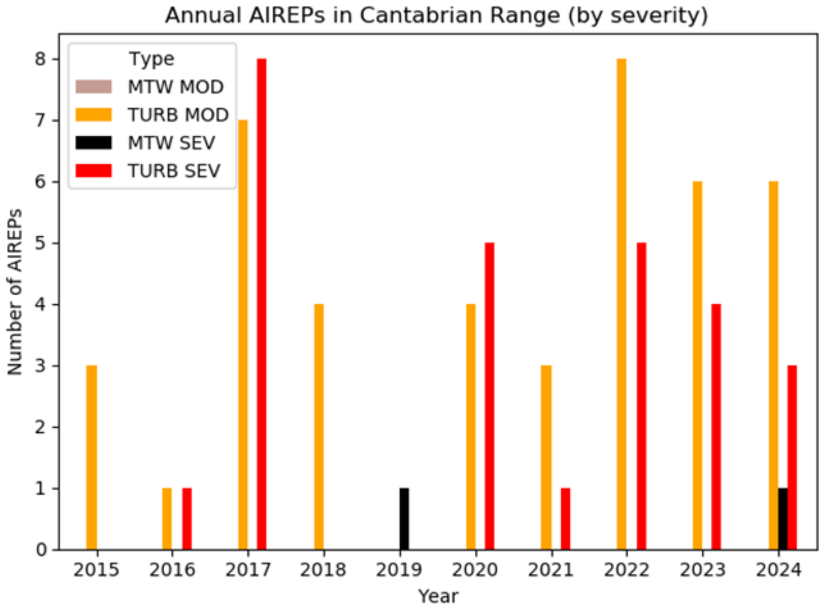

Figure 31. Annual AIREP record of turbulence and mountain wave in the Cantabrian mountain range, period 2014-2024.

At the monthly scale, Figure 32 and Table A-22 show that, due to the limited number of turbulence reports, the distribution of AIREPs appears to be relatively uniform throughout the year. March and November are the only months in which cases of severe mountain waves have been reported. In general, most events are clustered during the colder months (November to March), suggesting a certain seasonality associated with an increase in turbulence from various origins during the cold season.

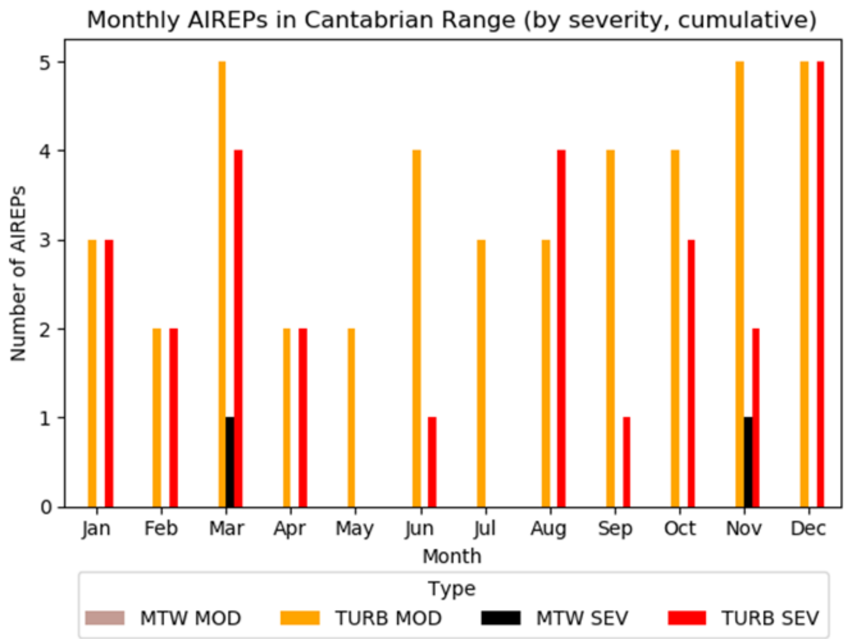

Figure 32. Monthly accumulated AIREP records of mountain waves and turbulence in the Cantabrian mountain range, period 2014-2024.

5.3 The Iberian System

The geographic polygon defined for the Iberian System mountain range has a perimeter of 1322 km and covers an area of 53 894 km². In order to characterise the synoptic situations that give rise to turbulence associated with mountain waves, this system is subdivided into two main sectors: the northwestern sector, which mainly includes border areas of Soria, La Rioja, and Burgos, and where prominent peaks exceeding 2000 metres are found, such as San Lorenzo (2271 m), Moncayo (2314 m), and Urbión (2228 m); and the southeastern sector, which mainly encompasses the provinces of Teruel and Castellón, as well as adjacent areas, where significant elevations are also found, such as Javalambre (2020 m), Peñarroya (2028 m), and Penyagolosa (1813 m). In both sectors, an atmospheric scenario favourable for the generation of mountain waves occurs under the presence of northwesterly low-level flows, typically associated with the rear flank of a trough, which provide favourable longitudinal shear for the development of wave structures. Furthermore, in the northwestern sector, ideal conditions for the formation of mountain waves may develop under southwesterly (*ábrego*) winds, especially when the flow acquires a certain degree of perpendicularity with respect to the dominant terrain.

It is important to note that convective activity also plays a significant role in the Iberian System, particularly in its southeastern sector. According to the climatology of lightning discharges in Spain developed by (Núñez *et al.*, 2019), this region contains one of the highest lightning density maxima in the Iberian Peninsula, located in the Maestrazgo area (Teruel-Castellón). This behaviour reflects a high frequency of convective episodes, particularly during the warm months, associated with atmospheric instability and the moisture supply provided by Mediterranean sea breezes, as well as with the interaction between dynamic forcing mechanisms and orographic effects. Consequently, this convective component may partially explain the recurrence of turbulence AIREPs in the Iberian System, especially during the summer months, reinforcing its status as one of the most active regions from an aeronautical perspective.

The area defined for the Iberian System combines relatively high activity with an intermediate severity percentage (34.2 %). This behaviour places it among the most relevant regions in terms of both frequency and intensity.

During the 2014-2024 period, Figure 33 and Table A-23 show that the Iberian System exhibits significant activity with regard to moderate turbulence, with an increasing trend interrupted by the COVID-19 pandemic and reaching an absolute maximum in 2024, with 38 reports. Other years with a high frequency of reports are 2018 (25) and 2021, 2022 (21 each). Severe turbulence has also been recurrent throughout the period, with notable peaks in 2019 (13 cases), 2023 (18), and 2024 (12). As for severe mountain waves, they have been recorded less frequently, with maximum values in 2019 (3) and 2017 (2), and a complete absence during the most recent years (from 2022 to 2024).

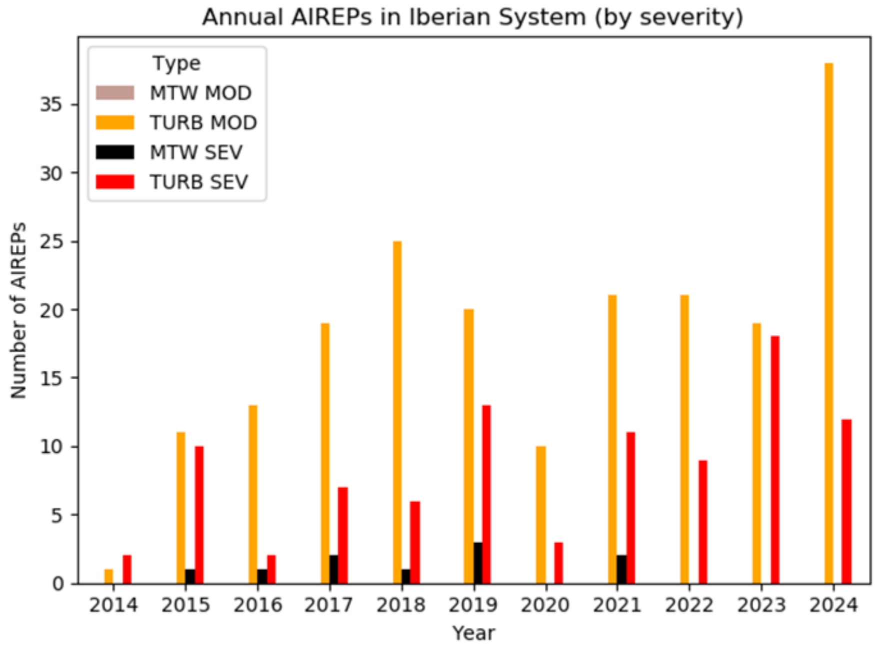

Figure 33. Annual AIREP record of turbulence and mountain waves in the Iberian System, period 2014-2024.

On a monthly basis, Figure 34 and Table A-24 show a clear concentration of reports during the winter quarter. January, February, and March are the months with the highest overall activity, accounting for more than 30% of the annual reports. In particular, February and March record the highest number of severe mountain wave events, while the period from October to March stands out for its high frequency of severe turbulence reports. In contrast, the period between May and August exhibits markedly lower activity. This monthly pattern indicates a strong influence of winter synoptic-scale dynamics on the Iberian System.

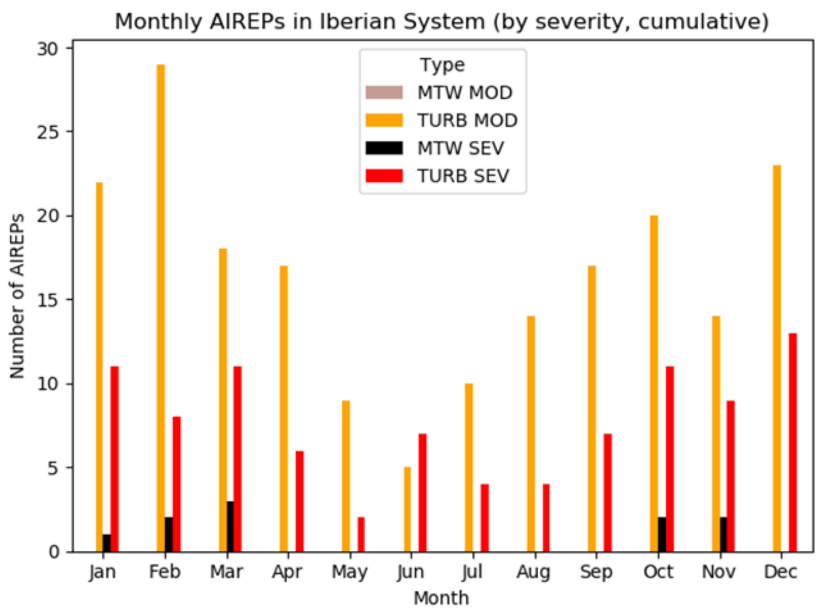

Figure 34. Monthly record of accumulated mountain wave and turbulence AIREPs in the Iberian System, 2014-2024 period.

5.4 The Central System

The geographical polygon defined for the Central System mountain range has a perimeter of 783 km and covers an area of 16 794 km². From the perspective of mountain wave generation, it can be divided into two sectors. The first extends zonally from west to east and includes the Sierra de Gredos, where several peaks exceed 2300 m, with Pico Almanzor reaching 2592 m as the highest summit. The same warm-sector scenario previously described for the Cantabrian Range gives rise to the so-called *abrego* winds, which are capable of generating turbulence associated with mountain waves on the lee side over the region of Castile and León.

The second sector is oriented approximately from southwest to northeast and is dominated by the Sierra de Guadarrama, where several peaks rise above 2200 m, with Peñalara (2428 m) being the highest elevation. A favourable scenario for mountain wave generation occurs under northwesterly flow impinging on the Segovian slope. At upper levels, this pattern is typically associated with the rear side of a trough, where confluent flow and subsidence prevail, stabilising the tropospheric column from upper to lower levels and potentially leading to the development of an inversion over the mountain range. Several studies have focused on the Sierra de Guadarrama because of its significant operational impact, as turbulence associated with mountain waves can affect the Madrid Terminal Maneuvering Area (TMA). Díaz-Fernández *et al*. (2022) analysed mountain wave episodes using the high-resolution HARMONIE-AROME model, assessing its ability to represent these phenomena in Spain and their implications for aviation safety.

Convective activity becomes moderately relevant during the warm season, favoured by daytime heating and orographic forcing. According to (Núñez *et al*., 2019), the density of lightning discharges in this region is moderate, reflecting the occurrence of locally developed diurnal thunderstorms. However, their impact shows a marked spatial dependence, being more significant in areas with higher air traffic density, such as the surroundings of the Sierra de Guadarrama. In general terms, the frequency of convection is lower than that observed in the Iberian System and the Pyrenees.

The adopted delimitation for the Central System exhibits the second-highest severity percentage (59.1 %), although based on a relatively small number of pilot reports (66). These reports are predominantly concentrated around the Sierra de Guadarrama, which may be related both to the higher density of air traffic in the area and to a potentially greater reporting proactivity among intermediaries within a reporting system that still presents certain inefficiencies.

During the 2014-2024 period, Figure 35 and Table A-25 show that the Central System exhibits a somewhat more significant level of activity regarding reports of severe mountain waves, with a total of 10 notifications. The year 2017 stands out with the highest number of cases, with four episodes recorded. During the remainder of the period, a lower frequency is observed, with a single case reported in 2018, 2019, 2022, and 2023, while two cases were recorded in 2024. No moderate mountain wave events were reported in any year. Regarding turbulence, moderate turbulence has been the most frequently reported category, showing a very marked increase in 2023 and especially in 2024, when 6 and 11 events were recorded, respectively. Severe turbulence has also displayed an upward trend in recent years, with notable peaks in 2023 (5 cases) and 2024 (9 cases).

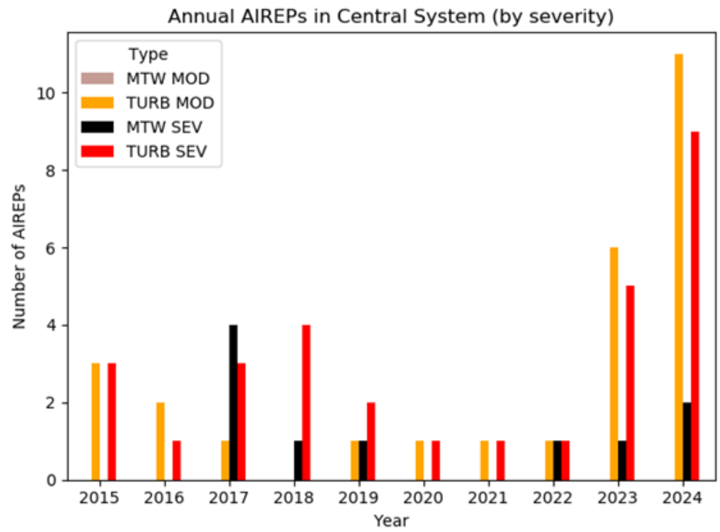

Figure 35. Annual record of turbulence and mountain wave AIREPs in the Central System, 2014-2024 period.

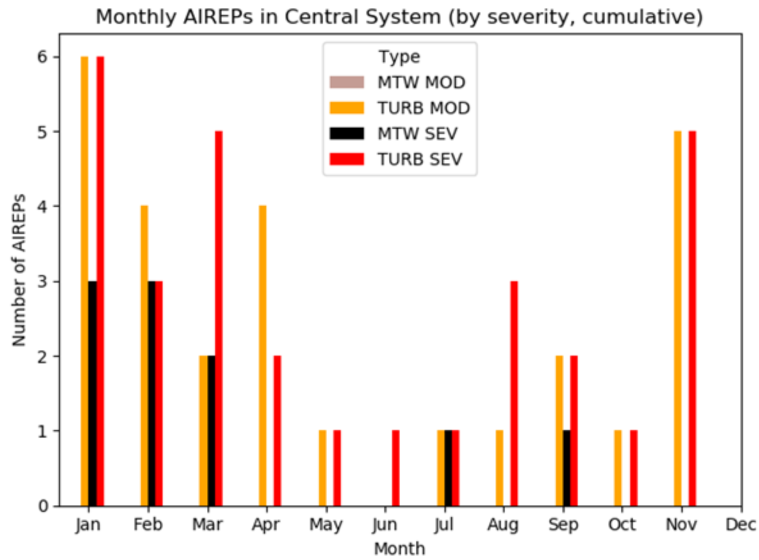

Figure 36. Monthly record of accumulated mountain wave and turbulence AIREPs in the Central System, 2014-2024 period.

From a monthly perspective, both Figure 36 and Table A-26 show that most notifications are concentrated during the winter months, with January being the month with the highest overall activity, recording a total of 15 reports. February and March also stand out due to the recurrent occurrence of severe mountain wave notifications, confirming a well-defined seasonal pattern: there is a greater tendency for the formation of intense orographic waves during the cold season. In contrast, during the warm months, particularly between May and July, AIREP activity is virtually negligible. This behaviour reflects the influence of winter synoptic-scale dynamics, characterised by the expansion and waviness of the circumpolar flow, which favours both the occurrence of turbulence from different origins and the establishment of conditions conducive to the development and vertical breaking of mountain waves.

5.5 The Betic System

The geographical polygon defined for the Betic System mountain range has a perimeter of 1055 km and covers an area of 46 366 km², making it the largest polygon in terms of spatial extent. It is subdivided into the Prebetic, Subbetic, and Penibetic ranges, the latter containing the highest elevations above 3000 m in the Sierra Nevada, where Mulhacén (3479 m) stands as the highest peak of the Iberian Peninsula.

The polygon selected to represent the Betic System records the highest total number of pilot reports among all the areas analysed. However, the proportion of severe phenomena is the lowest (12.4 %), indicating that although turbulence is frequent, moderate intensity clearly predominates. This behaviour may suggest that the dynamical processes responsible for generating turbulence in this region are generally less critical from an operational perspective.

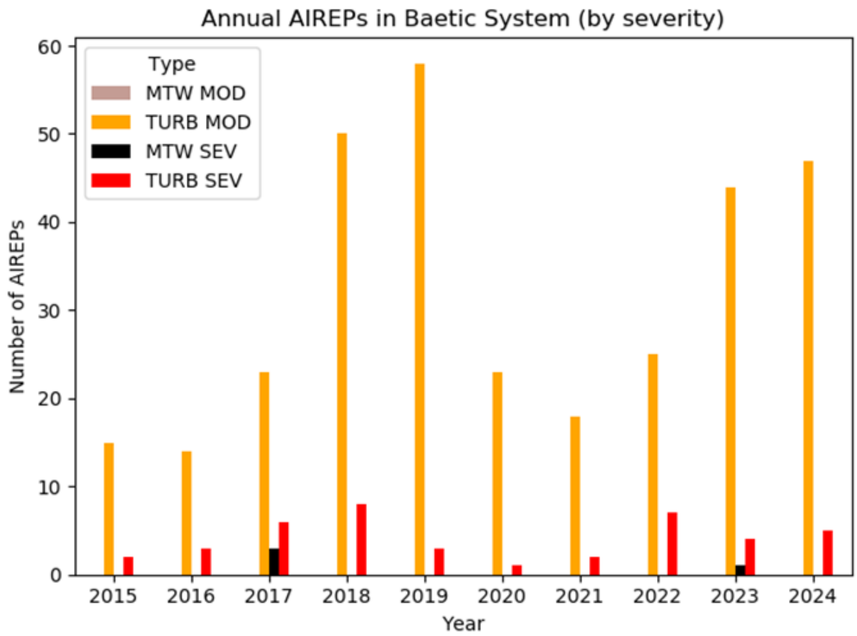

Figure 37. Annual record of turbulence and mountain wave AIREPs in the Betic System, 2014-2024 period.

During the 2015-2024 period, Figure 37 and Table A-27 indicate that the Betic System has exhibited a high frequency of moderate turbulence reports, particularly from 2017 onwards, showing an increasing trend interrupted by the COVID-19 pandemic in 2020 and reaching maxima in 2019 (58 cases), 2018 (50 cases), and 2024 (47 cases). Severe turbulence, although less frequent, has been present throughout the entire period with moderate values, with notable peaks in 2018 (8 cases), 2017 (6 cases), and 2022 (7 cases). Regarding severe mountain waves, their occurrence has been sporadic and limited to only a few years: 2017 (3 cases) and 2023 (1 case). No moderate-intensity mountain wave reports were recorded.

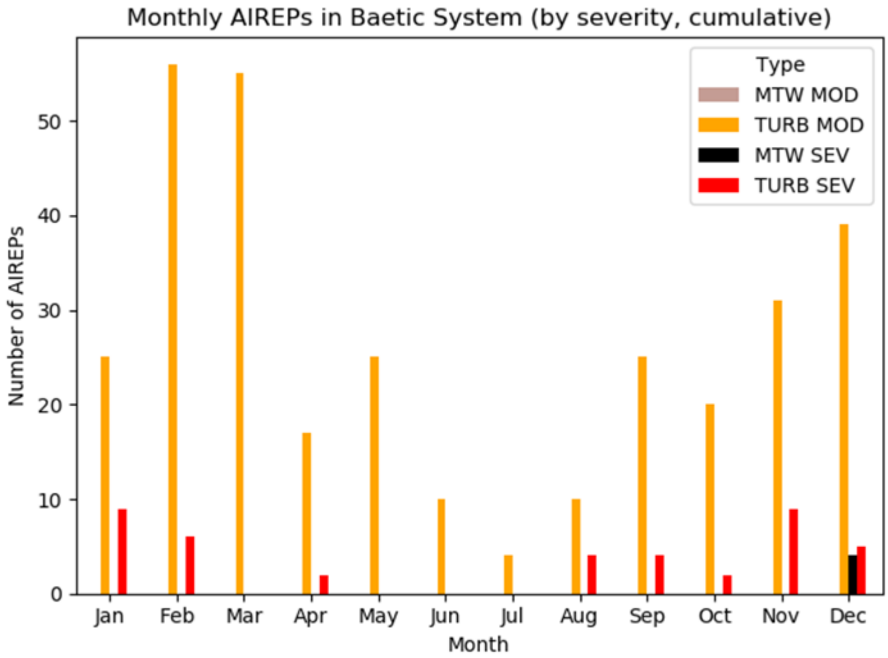

Figure 38. Monthly record of accumulated mountain wave and turbulence AIREPs in the Betic System, 2014-2024 period.

On a monthly basis, Figure 38 and Table A-28 show a very pronounced seasonal pattern: the highest volume of AIREPs is concentrated between January and March, with February and March recording the greatest number of reports (62 and 55, respectively). However, severe mountain wave events were observed exclusively in December, when four cases were recorded. Peaks in severe turbulence are also evident in January (9 cases) and November (9 cases), suggesting that the transition and winter months are more conducive to the development of conditions favourable for orographic turbulence. In contrast, activity between June and August is minimal, reflecting the clear influence of winter synoptic-scale circulation on the genesis of these phenomena.

6. CONCLUSIONS

The present analysis of AIREPs (ARS) issued between 2014 and 2024 within the Madrid, Barcelona, and Canary Islands FIRs has provided a detailed overview of the temporal and spatial behaviour of turbulence and icing phenomena, both of moderate (MOD) and severe (SEV) intensity, as well as their relationship with the orography of the main mountain ranges of the Iberian Peninsula. Based on the results obtained, the following main conclusions can be drawn:

1. Inherent limitation due to the subjectivity of AIREPs

AIREPs depend on pilots' subjective perception, the characteristics of the aircraft, and the phase of flight, which introduces certain biases in intensity reporting and uncertainties in their spatial and temporal positioning. Therefore, although they constitute a very valuable source of information, their results must be interpreted with caution and complemented with other observation and modelling systems.

2. High geographical concentration in the Madrid and Barcelona FIRs

94.8 % of the reports are located within the Madrid and Barcelona FIRs. The Canary Islands FIR accounts for a low density of AIREPs (5.2 %), suggesting limitations in observation or data transmission that may depend on the configuration of air traffic in this region.

3. Sustained increase in reports after the pandemic

Over the last decade, there has been an increase in the total number of AIREPs, which was interrupted by the impact of the COVID-19 pandemic in 2020. This trend is observed in both moderate and severe phenomena, with maxima tending to occur in 2024. This pattern is strongly related to air traffic volume.

4. Decoupling between AIREP distribution and meteorological reality

The spatial distribution of AIREPs is strongly conditioned by air traffic density, meaning that it does not necessarily represent the actual distribution of meteorological phenomena. This bias limits their direct use for climatological studies and reinforces the need to combine these observations with numerical models and other independent data sources.

5. Predominance of turbulence over icing

Turbulence is the most frequently reported phenomenon in the analysed AIREP dataset, especially in its moderate form. In comparison, icing is less frequent, although it also shows an increasing trend, particularly in the last years of the analysed period.

6. Marked seasonality

Most reports are concentrated in the cold months (December to March), for both turbulence and icing. This pattern is driven, in the case of turbulence, by the intensification and equatorward shift of jet streams in winter (favouring CAT and wind shear). In the case of icing, it is associated with active frontal systems and cold, moist air masses, which favour icing at low and mid levels. The concentration of AIREPs during the summer period is mainly linked to convective phenomena. Their highly localised nature, both spatially and temporally, explains the lower reporting frequency compared with other seasons. Nevertheless, these phenomena can have a high impact on air traffic management, making accurate monitoring and forecasting essential to enhance operational safety and mitigate associated economic impacts.

7. Distinct characteristic altitudes

Turbulence is predominantly reported between FL300-FL390, consistent with the position of the polar jet streams. In the Barcelona FIR, a greater vertical dispersion of reports is also observed compared with the Madrid FIR, likely associated with stronger convective activity due to moisture influx from the Mediterranean and orographic processes. Icing is concentrated between FL100-FL220, although in summer a higher vertical spread occurs as a result of strong updrafts associated with convective processes. Likewise, during the warm months in the Madrid FIR, reports are observed at higher altitudes compared with the Barcelona FIR. This difference may be explained by the presence of dry and warm air over the Iberian interior during this period, which raises both cloud bases and the freezing level.

8. Underrepresentation of mountain waves

AIREPs explicitly identified as "MTW" are scarce. However, the geographical and seasonal analysis shows that many turbulence episodes reported as "TURB" could have an orographic origin. This subjectivity in pilot coding limits the precise identification of the phenomenon.

9. Significant orographic influence

The main mountain systems show a clear seasonality in the reports, with maxima in winter, when the interaction between airflow and terrain under stable and sheared conditions favours the generation of mountain waves and severe orographic turbulence.

The combined analysis reveals a clear contrast between the frequency and intensity of the phenomena. While the Betic System concentrates the highest number of pilot reports, these are mostly of moderate intensity. In contrast, the Pyrenees, the Cantabrian Range, and the Central System, although showing a lower number of cases, present a significantly higher proportion of severe phenomena, making them the regions with the greatest potential risk. The Iberian System occupies an intermediate position, combining relatively high activity with moderate severity.

Overall, these results highlight the importance of considering not only the frequency of events but also their intensity, with the Pyrenees being the most relevant mountain system from an operational perspective in terms of hazard.

10. Need for operational and methodological improvements

Given the high volume of air traffic and the frequency of turbulence and icing related events, it is recommended to optimise AIREP collection and transmission procedures, moving towards more automated systems. Over this 11-year study period, the number of reports in Spanish airspace has been relatively low, which limits the capacity for analysis and response to these phenomena. To put the low number of reports into context relative to the number of operations, in 2024 alone, 2.3 million flights were handled according to a press release from ENAIRE (2025).

To this end, it is necessary to promote meteorological training for pilots and ACC personnel in order to improve the coding of orographic phenomena (MTW vs TURB). Therefore, improving both the systematisation and frequency of reports would significantly contribute to enhancing operational safety, as well as improving the quality of meteorological monitoring and, consequently, strategic decision-making in the aviation domain.

11. Potential future research directions

First, this study opens the door to a comprehensive analysis of the synoptic and mesoscale scenarios that give rise to the meteorological phenomena responsible for these observations. Future work should focus on systematically identifying such scenarios and establishing recurrent patterns. Likewise, it would be relevant to develop automated methodologies that quantitatively relate synoptic and mesoscale conditions to the frequency and intensity of observed events, thereby improving the understanding of the atmospheric processes involved and ultimately optimising forecasting and monitoring strategies.

Second, despite their limitations, AIREPs constitute one of the few direct sources of in-flight observations, making them a fundamental tool for developing automatic processes to validate or verify turbulence and icing prediction products, especially in environments where remote sensing has limitations.

Finally, integrating AIREPs with other airborne observational sources (AMDAR and SSR Mode-S) opens a promising line for the development of post-processing machine learning techniques capable of calibrating and improving turbulence and icing indices, reducing the uncertainty associated with numerical models.

Overall, this study highlights the strategic value of AIREPs within the aeronautical meteorological monitoring system, not only as a diagnostic tool but also as a key component for the development of new, more accurate, integrated, and continuously improving prediction methodologies aimed at enhancing operational safety.

7. REFERENCES

AEMET (2012). *Pronóstico de engelamiento y ondas de montaña mediante teledetección y modelos*. 6º Simposio Nacional de Predicción, Agencia Estatal de Meteorología, Madrid. Available at: https://repositorio.aemet.es

AENA (2025). Air traffic statistics of Spanish airports. AENA, Madrid. Available at: https://www.aena.es/es/estadisticas/inicio.html

Belo-Pereira, M. (2015). Comparison of in-flight aircraft icing algorithms based on ECMWF forecasts. *Meteorological Applications*, 22, 705–715. https://doi.org/10.1002/met.1505

Belo-Pereira, M. (2022). Aviation Turbulence Forecasting over the Portuguese Flight Information Regions: Algorithm and Objective Verification. *Atmosphere*, 13(3), 422.

Clark, T. L., and Peltier, W. R. (1977). On the Evolution and Stability of Finite-Amplitude Mountain Waves. *Journal of the Atmospheric Sciences*, 34, 1715–1730.

Clark, T. L., and Peltier, W. R. (1983). Nonlinear Mountain Waves in Two and Three Spatial Dimensions. *Quarterly Journal of the Royal Meteorological Society*, 109, 527–554.

Clem, L. H. (1955). Clear-Air Turbulence Near the Jet-Stream Maxima. *Bulletin of the American Meteorological Society*, 36(2), 53–60.

Cuevas, E. (2001). *Variabilidad del chorro subtropical y su influencia en la atmósfera sobre Canarias*. Instituto Nacional de Meteorología (INM), Centro de Investigación Atmosférica de Izaña.

Díaz-Fernández, J., Quitián-Hernández, L., Santos-Muñoz, D., Fernández-González, S., Valero, F., Merino, A., García-Ortega, E., Sánchez, J. L., Sastre, M., and Martín, M. L. (2022). Mountain wave episodes using the high-resolution HARMONIE-AROME model in Spain. Preprint. Available at: https://arxiv.org/abs/2205.00109

Eick, D. (2015a). Aircraft Icing Accidents. Presentation at the NCAR In-flight Icing Users Technical Interchange Meeting (TIM), Washington, D.C., February 2015. National Transportation Safety Board (NTSB), Office of Aviation Safety. Available at: https://ral.ucar.edu/sites/default/files/docs//eick-ntsb-ncar-icing-presentation.pdf

Eick, D. (2015b). Turbulence-Related Accidents and Incidents. National Transportation Safety Board (NTSB) / UCAR–NCAR Research Applications Laboratory (RAL). Available at: https://ral.ucar.edu/sites/default/files/docs/eick-turbulencerelatedaccidents.pdf

ENAIRE (2025). ENAIRE achieves its best historical record: more than 2.3 million flights managed in 2024. ENAIRE, Press release, 15 January 2025. Available at: https://www.enaire.es/es_ES/2025_01_15/ndp_enaire_logra_mejor_registro_historico_mas_2_millones_vuelos

EUMETSAT (2004). Case study: Mountain waves – Spain and the Balearic Islands, 28 December 2004. EUMETSAT Case Studies, Darmstadt. Available at: https://www.eumetsat.int

Fernández-González, S., Sánchez, J. L., Gascón, E., López, L., García-Ortega, E., and Merino, A. (2014). Weather features associated with aircraft icing conditions: a case study. *The Scientific World Journal*, 2014, Article ID 279063, 18 pp.

Font Tullot, I. (1956). *El tiempo atmosférico en las Islas Canarias*. Instituto Nacional de Meteorología (actual AEMET).

Hermoso, A., Rivière, G., Harvey, B., Methven, J., & Schemm, S. (2024). A dynamical interpretation of the intensification of the North Atlantic jet. *Journal of Climate*.

Jansà, A., Monserrat, S., and Gomis, D. (2007). The rissaga of 15 June 2006 in Ciutadella (Menorca), a meteorological tsunami. *Advances in Geosciences*, 12, 1–4.

Núñez Mora, J. Á., Riesco Martín, J., and Mora García, M. A. (2019). *Climatología de descargas eléctricas y de días de tormenta en España*. Agencia Estatal de Meteorología (AEMET). Available at: https://repositorio.aemet.es/

UCAR/COMET (2012). *Dominio del diagrama oblicuo T – log p.* MetEd: Meteorology Education and Training. University Corporation for Atmospheric Research (UCAR), Boulder, Colorado. Available at: https://www.meted.ucar.edu

UCAR/COMET (2014). Mountain Waves and Downslope Winds. MetEd: Meteorology Education and Training. University Corporation for Atmospheric Research (UCAR), Boulder, Colorado. Available at: https://www.meted.ucar.edu

UCM–AEMET (2022). *Climatología de ondas de montaña en la Sierra de Guadarrama*. Agencia Estatal de Meteorología (AEMET) and Universidad Complutense de Madrid. Available at: https://repositorio.aemet.es

Wen, Y., Wang, C., Wang, Z., Wang, R., and Yuan, M. (2025). Analysis of the characteristics of four severe aircraft icing events in Southwest China during the winter of 2023. *Frontiers in Earth Science,* 13, 1586116. https://doi.org/10.3389/feart.2025.1586116

8. ANNEX

YEAR	ICE MOD	TURB MOD	ICE SEV	TURB SEV
2014	2	5	0	5
2015	42	133	11	61
2016	26	136	10	68
2017	33	189	7	137
2018	94	414	18	150
2019	79	430	31	153
2020	44	217	10	86
2021	64	282	14	75
2022	100	379	15	100
2023	114	456	28	149
2024	168	559	19	172

Table A-1. AIREP records for the Madrid, Barcelona and Canary Islands FIRs, period 2014-2024.

YEAR	ICE MOD	TURB MOD	ICE SEV	TURB SEV
2014	0	4	0	2
2015	23	84	5	22
2016	11	89	7	26
2017	12	137	5	75
2018	24	222	5	70
2019	34	196	19	51
2020	19	107	5	36
2021	16	114	10	38
2022	42	160	8	40
2023	63	192	20	80
2024	74	269	14	97

Table A-2. Annual AIREP record for the Madrid FIR, period 2014-2024.

YEAR	ICE MOD	TURB MOD	ICE SEV	TURB SEV
2014	2	1	0	3
2015	19	48	6	39
2016	15	37	3	37
2017	21	49	2	55
2018	69	188	12	74
2019	45	234	12	98
2020	24	110	5	42
2021	47	168	3	36
2022	55	218	6	51
2023	50	185	7	60
2024	84	198	5	62

Table A-3. Annual AIREP record for the Barcelona FIR, period 2014-2024.

YEAR	ICE MOD	TURB MOD	ICE SEV	TURB SEV
2015	0	1	0	0
2016	0	10	0	5
2017	0	3	0	7
2018	1	4	1	6
2019	0	0	0	4
2020	1	0	0	8
2021	1	0	1	1
2022	3	1	1	9
2023	1	79	1	9
2024	10	92	0	13

Table A-4. Annual AIREP record for the Canary Islands FIR, period 2014-2024.

YEAR	ICE MOD	TURB MOD	ICE SEV	TURB SEV
JANUARY	96	335	31	176
FEBRUARY	65	390	21	124
MARCH	93	442	13	122
APRIL	66	257	3	78
MAY	56	210	10	38
JUNE	27	140	7	54
JULY	13	145	4	44
AUGUST	24	150	2	62
SEPTEMBER	55	231	9	91
OCTOBER	88	235	13	92
NOVEMBER	94	269	31	133
DECEMBER	88	390	19	142

Table A-5. AIREP records for the Madrid, Barcelona and Canary Islands FIRs, period 2014-2024.

YEAR	ICE MOD	TURB MOD	ICE SEV	TURB SEV
JANUARY	36	176	20	81
FEBRUARY	28	229	10	55
MARCH	34	226	10	54
APRIL	20	111	3	28
MAY	18	87	7	15
JUNE	14	47	5	28
JULY	5	58	3	24
AUGUST	15	60	2	30
SEPTEMBER	19	111	4	37
OCTOBER	44	132	7	61
NOVEMBER	43	147	14	57
DECEMBER	42	190	13	67

Table A-6. Monthly AIREP record for the Madrid FIR, period 2014-2024.

YEAR	ICE MOD	TURB MOD	ICE SEV	TURB SEV
JANUARY	60	143	11	83
FEBRUARY	37	140	11	54
MARCH	57	192	3	60
APRIL	45	117	0	49
MAY	37	97	3	20
JUNE	13	78	2	24
JULY	7	87	0	19
AUGUST	7	84	0	32
SEPTEMBER	35	120	5	53
OCTOBER	43	96	6	30
NOVEMBER	48	116	14	71
DECEMBER	42	166	6	61

Table A-7. Monthly AIREP record for the Barcelona FIR, period 2014-2024.

YEAR	ICE MOD	TURB MOD	ICE SEV	TURB SEV
JANUARY	0	16	0	11
FEBRUARY	0	21	0	15
MARCH	2	24	0	8
APRIL	1	29	0	1
MAY	1	26	0	3
JUNE	0	15	0	2
JULY	1	0	1	1
AUGUST	2	6	0	0
SEPTEMBER	1	4	0	1
OCTOBER	2	9	0	1
NOVEMBER	3	6	3	5
DECEMBER	4	34	0	14

Table A-8. Monthly AIREP record for the Canary Islands FIR, period 2014-2024.

MONTH	Median altitude FL	Min altitude FL	Max altitude FL	No. of AIREPs
JANUARY	350	0	493	510
FEBRUARY	350	0	457	510
MARCH	330	5	430	561
APRIL	330	5	502	334
MAY	340	20	450	245
JUNE	310	0	500	191
JULY	290	27	410	189
AUGUST	330	0	643	212
SEPTEMBER	330	0	533	325
OCTOBER	330	10	410	329
NOVEMBER	340	0	430	400
DECEMBER	350	8	430	528

Table A-9. Monthly record of turbulence at flight levels (FL), period 2014-2024.

MONTH	Median altitude FL	Min altitude FL	Max altitude FL	No. of AIREPs
JANUARY	360	10	410	257
FEBRUARY	350	50	457	282
MARCH	340	5	430	278
APRIL	340	80	502	138
MAY	350	40	390	102
JUNE	330	70	430	75
JULY	350	60	410	82
AUGUST	360	30	643	90
SEPTEMBER	350	10	400	148
OCTOBER	350	30	400	193
NOVEMBER	350	0	430	202
DECEMBER	350	10	430	256

Table A-10. Monthly record of turbulence at flight levels (FL) in the Madrid FIR, period 2014-2024.

MONTH	Median altitude FL	Min altitude FL	Max altitude FL	No. of AIREPs
JANUARY	335	0	430	226
FEBRUARY	340	0	430	192
MARCH	300	10	410	251
APRIL	310	20	410	166
MAY	310	20	400	115
JUNE	210	0	500	102
JULY	115	27	400	106
AUGUST	185	0	400	116
SEPTEMBER	250	0	533	172
OCTOBER	235	10	410	126
NOVEMBER	300	0	420	187
DECEMBER	330	8	430	226

Table A-11. Monthly record of turbulence at flight levels (FL) in the Barcelona FIR, period 2014-2024.

MONTH	Median altitude FL	Min altitude FL	Max altitude FL	No. of AIREPs
JANUARY	330	70	493	27
FEBRUARY	350	140	400	36
MARCH	340	5	410	32
APRIL	330	5	400	30
MAY	330	5	450	28
JUNE	355	45	430	14
JULY	80	80	80	1
AUGUST	215	90	300	6
SEPTEMBER	330	120	380	5
OCTOBER	270	110	380	10
NOVEMBER	130	19	390	11
DECEMBER	350	40	400	46

Table A-12. Monthly record of turbulence at flight levels (FL) in the Canary Islands FIR, period 2014-2024.

MONTH	Median altitude FL	Min altitude FL	Max altitude FL	No. of AIREPs
JANUARY	150	10	500	127
FEBRUARY	130	50	360	85
MARCH	140	50	380	105
APRIL	110	40	270	69
MAY	150	100	330	66
JUNE	180	120	330	34
JULY	200	100	380	17
AUGUST	180	90	340	26
SEPTEMBER	180	20	370	63
OCTOBER	190	80	450	101
NOVEMBER	160	40	340	125
DECEMBER	180	10	390	106

Table A-13. Monthly record of icing at flight levels (FL), period 2014-2024.

MONTH	Median altitude FL	Min altitude FL	Max altitude FL	No. of AIREPs
JANUARY	150	10	370	56
FEBRUARY	150	80	360	37
MARCH	150	60	360	43
APRIL	120	70	250	23
MAY	150	100	250	25
JUNE	190	120	330	19
JULY	220	180	380	8
AUGUST	180	120	340	17
SEPTEMBER	180	100	370	23
OCTOBER	200	90	450	50
NOVEMBER	160	60	260	57
DECEMBER	180	10	390	54

Table A-14. Monthly record of icing at flight levels (FL) in the Madrid FIR, period 2014-2024.

MONTH	Median altitude FL	Min altitude FL	Max altitude FL	No. of AIREPs
JANUARY	140	30	500	71
FEBRUARY	105	50	310	48
MARCH	125	50	380	60
APRIL	110	40	210	45
MAY	150	100	330	40
JUNE	170	120	330	15
JULY	150	100	210	7
AUGUST	170	90	330	7
SEPTEMBER	180	20	350	39
OCTOBER	180	80	340	49
NOVEMBER	160	40	270	62
DECEMBER	180	60	380	48

Table A-15. Monthly records of icing at flight levels (FL) in the Barcelona FIR, period 2014-2024.

MONTH	Mean altitude FL	Min altitude FL	Max altitude FL	No. of AIREPs
JANUARY	---	---	---	0
FEBRUARY	---	---	---	0
MARCH	110	110	110	2
APRIL	270	270	270	1
MAY	100	100	100	1
JUNE	---	---	---	0
JULY	220	190	250	2
AUGUST	195	190	200	2
SEPTEMBER	230	230	230	1
OCTOBER	210	210	210	2
NOVEMBER	205	80	340	6
DECEMBER	170	140	190	4

Table A-16. Monthly record of icing at flight levels (FL) in the Canary Islands FIR, period 2014-2024.

YEAR	MTW MOD	TURB MOD	MTW SEV	TURB SEV
2014	0	1	0	2
2015	0	35	2	29
2016	0	33	1	14
2017	0	51	13	39
2018	2	91	10	34
2019	0	88	13	30
2020	0	40	0	16
2021	2	59	4	17
2022	0	71	6	34
2023	0	82	3	36
2024	0	112	4	48

Table A-17. Annual record of mountain-wave and turbulence AIREPs for all mountain systems, period 2014-2024.

MONTH	MTW MOD	TURB MOD	MTW SEV	TURB SEV
JANUARY	0	66	10	54
FEBRUARY	0	99	9	31
MARCH	0	87	11	28
APRIL	0	50	2	27
MAY	0	41	3	7
JUNE	2	23	0	9
JULY	0	18	0	6
AUGUST	0	37	1	15
SEPTEMBER	0	53	1	23
OCTOBER	0	55	4	20
NOVEMBER	0	55	4	35
DECEMBER	2	79	11	44

Table A-18. Monthly record of turbulence and mountain-wave AIREPs for all mountain systems, period 2014-2024.

YEAR	MTW MOD	TURB MOD	MTW SEV	TURB SEV
2014	0	0	0	0
2015	0	3	1	14
2016	0	3	0	7
2017	0	1	4	15
2018	2	12	8	16
2019	0	9	8	12
2020	0	2	0	6
2021	2	16	2	2
2022	0	16	5	12
2023	0	7	1	5
2024	0	10	1	19

Table A-19. Annual record of mountain-wave and turbulence AIREPs for the Pyrenees, period 2014-2024.

MONTH	MTW MOD	TURB MOD	MTW SEV	TURB SEV
JANUARY	0	10	6	25
FEBRUARY	0	8	4	12
MARCH	0	7	5	8
APRIL	0	10	2	15
MAY	0	5	3	5
JUNE	2	3	0	0
JULY	0	1	0	1
AUGUST	0	9	0	2
SEPTEMBER	0	6	1	8
OCTOBER	0	9	1	2
NOVEMBER	0	4	1	14
DECEMBER	2	7	7	16

Table A-20. Monthly record of turbulence and mountain-wave AIREPs for the Pyrenees, period 2014-2024.

YEAR	MTW MOD	TURB MOD	MTW SEV	TURB SEV
2014	0	0	0	0
2015	0	3	0	0
2016	0	1	0	1
2017	0	7	0	8
2018	0	4	0	0
2019	0	0	1	0
2020	0	4	0	5
2021	0	3	0	1
2022	0	8	0	5
2023	0	6	0	4
2024	0	6	1	3

Table A-21. Annual record of mountain-wave and turbulence AIREPs for the Cantabrian Mountains, period 2014-2024.

MONTH	MTW MOD	TURB MOD	MTW SEV	TURB SEV
JANUARY	0	3	0	3
FEBRUARY	0	2	0	2
MARCH	0	5	1	4
APRIL	0	2	0	2
MAY	0	2	0	0
JUNE	0	4	0	1
JULY	0	3	0	0
AUGUST	0	3	0	4
SEPTEMBER	0	4	0	1
OCTOBER	0	4	0	3
NOVEMBER	0	5	1	2
DECEMBER	0	5	0	5

Table A-22. Monthly record of turbulence and mountain-wave AIREPs for the Cantabrian Mountains, period 2014-2024.

YEAR	MTW MOD	TURB MOD	MTW SEV	TURB SEV
2014	0	1	0	2
2015	0	11	1	10
2016	0	13	1	2
2017	0	19	2	7
2018	0	25	1	6
2019	0	20	3	13
2020	0	10	0	3
2021	0	21	2	11
2022	0	21	0	9
2023	0	19	0	18
2024	0	38	0	12

Table A-23. Annual record of mountain-wave and turbulence AIREPs for the Iberian System, period 2014-2024.

MONTH	MTW MOD	TURB MOD	MTW SEV	TURB SEV
JANUARY	0	22	1	11
FEBRUARY	0	29	2	8
MARCH	0	18	3	11
APRIL	0	17	0	7
MAY	0	9	0	2
JUNE	0	5	0	7
JULY	0	10	0	4
AUGUST	0	14	0	4
SEPTEMBER	0	17	0	7
OCTOBER	0	20	2	11
NOVEMBER	0	14	2	9
DECEMBER	0	23	0	13

Table A-24. Monthly record of turbulence and mountain-wave AIREPs for the Iberian System, period 2014-2024.

YEAR	MTW MOD	TURB MOD	MTW SEV	TURB SEV
2014	0	0	0	0
2015	0	3	0	3
2016	0	2	0	1
2017	0	1	4	3
2018	0	0	1	4
2019	0	1	1	2
2020	0	1	0	1
2021	0	1	0	1
2022	0	1	1	1
2023	0	6	1	5
2024	0	11	2	9

Table A-25. Annual record of mountain-wave and turbulence AIREPs for the Central System, period 2014-2024.

MONTH	MTW MOD	TURB MOD	MTW SEV	TURB SEV
JANUARY	0	6	3	6
FEBRUARY	0	4	3	3
MARCH	0	2	2	5
APRIL	0	4	0	2
MAY	0	0	0	0
JUNE	0	1	0	1
JULY	0	0	0	1
AUGUST	0	1	1	1
SEPTEMBER	0	1	0	3
OCTOBER	0	2	1	2
NOVEMBER	0	1	0	1
DECEMBER	0	5	0	5

Table A-26. Monthly record of turbulence and mountain-wave AIREPs for the Central System, period 2014-2024.

YEAR	MTW MOD	TURB MOD	MTW SEV	TURB SEV
2014	0	0	0	0
2015	0	15	0	2
2016	0	14	0	3
2017	0	23	3	6
2018	0	50	0	8
2019	0	58	0	3
2020	0	23	0	1
2021	0	18	0	2
2022	0	25	0	7
2023	0	44	1	4
2024	0	47	0	5

Table A-27. Annual record of mountain-wave and turbulence AIREPs for the Betic System, period 2014-2024.

MONTH	MTW MOD	TURB MOD	MTW SEV	TURB SEV
JANUARY	0	25	0	9
FEBRUARY	0	56	0	6
MARCH	0	55	0	0
APRIL	0	17	0	2
MAY	0	25	0	0
JUNE	0	10	0	0
JULY	0	4	0	0
AUGUST	0	10	0	4
SEPTEMBER	0	25	0	4
OCTOBER	0	20	0	2
NOVEMBER	0	31	0	9
DECEMBER	0	39	4	5

Table A-28. Monthly record of turbulence and mountain-wave AIREPs for the Betic System, period 2014-2024.